



Shuvo Das

PWM Driven LEDs Based on Isolated DC Voltage Measurement

Metropolia University of Applied Sciences

Bachelor of Engineering

Electronics

Bachelor's Thesis

15 September 2023

Abstract

Author: Shuvo Das
Title: PWM Driven LEDs Based on Isolated DC Voltage Measurement
Number of Pages: 72 pages + 1 appendix
Date: 15 September 2023

Degree: Bachelor of Engineering
Degree Programme: Electronics
Supervisors: Riya Sindhwani, Senior Lecturer
Juuso Sakkara, Head of the Design Team

Voltage regulated LED driver ICs are commonly used to drive LEDs in variable voltage conditions. The purpose of this thesis work was to design an LED driving circuit without using LED driver ICs for Teknoware company. A PWM controlled average current method was used to cope with the variability of the voltage source. The LEDs are operated in switch mode by a microcontroller generated PWM signals through an isolation barrier. The brightness levels are controlled by varying the duty cycles of the PWM signals. The microcontroller measures the power supply voltage through the isolation barrier and determines appropriate PWM duty cycles to attain specific brightness levels. The average current regulation was designed for 21V to 30V. The 3000K and 5000K color temperature LEDs were used in the circuit. The 5000K LEDs have emergency current paths in the event of missing PWM signal.

Different techniques for the isolated DC voltage measurement were explored, such as linear optocoupler, isolation amplifier based techniques. A PWM based voltage measurement circuit was developed to provide a lower cost solution. The company continued with a TL431 based voltage measurement circuit at the end. The voltage measurement circuits were measured twice; the second measurements were taken by changing ICs with the same models to observe how IC to IC variation affects the measurement accuracy. The linear optocoupler based circuit had the largest voltage measurement error, while the isolation amplifier based circuit provided the best measurement accuracy. TL431 based circuit produced a maximum 676mV difference with the power supply voltage between 20V and 30V, whereas the PWM based voltage measurement circuit produced a maximum of 375mV difference.

The measured PWM duty cycles for different brightness levels and emergency mode current were close to the theoretical values.

The software department of the company utilizes the result of this thesis work to program the microcontroller for driving the LEDs.

Keywords: Isolated voltage measurement, optocoupler, PWM

The originality of this thesis has been checked using Turnitin Originality Check service.

Contents

List of Abbreviations

1	Introduction	1
2	Theoretical Background	3
2.1	Isolation	3
2.2	PWM Generation	8
2.3	PWM to DC Voltage	10
2.4	Op-amp Circuits	17
2.5	TL431	18
2.6	LED Circuits	19
2.6.1	Single Transistor Based CC	19
2.6.2	Two Transistors Based CC	22
2.6.3	Op-amp and Transistor Based CC	23
2.6.4	Switch Mode	24
3	Circuits Description	26
3.1	Isolated DC Voltage Measurement Circuits	26
3.1.1	Linear Optocoupler Based Voltage Measurement	27
3.1.2	Isolation Amplifier Based Voltage Measurement	29
3.1.3	TL431 Based Voltage Measurement	30
3.1.4	PWM Based Voltage Measurement	31
3.2	LED Circuits	39
3.2.1	3000K LED Channel	39
3.2.2	5000K LED Channel	43
4	Results	45
4.1	Isolated DC Voltage Measurement Circuits	45
4.1.1	Linear Optocoupler Based Voltage Measurement	45
4.1.2	Isolation Amplifier Based Voltage Measurement	46
4.1.3	TL431 Based Voltage Measurement	47
4.1.4	PWM Based Voltage Measurement	49
4.2	LED Circuits	55
4.2.1	3000K LED Channel	55
4.2.2	5000K LED Channel	58

5	Discussion	62
6	Conclusion	66
	References	70

Appendices

Appendix 1: Additional PWM Based Voltage Measurement Results

List of Abbreviations

ADC Analog to Digital Converter

CC Constant Current

DC Direct Current

IC Integrated Circuit

LED Light Emitting Diode

LPF Low Pass Filter

MOSFET Metal Oxide Semiconductor Field Effect Transistor

PCB Printed Circuit Board

PWM Pulse Width Modulation

1 Introduction

This thesis discusses the design and implementation of an LED card for Teknoware company. Teknoware provides lighting solutions to public transport such as buses, trains, trams. Here, an LED card refers to the single unit of a lighting solution. The number of LEDs on an LED card depends on the target lumen level. A lighting solution is equipped with many LED cards, and all LED cards are powered by the same direct current (DC) voltage source. The DC voltage source is variable, but the LED cards are required to provide the same lumen output. The use of voltage regulated LED drivers is one of the methods for driving the LEDs in variable DC voltage conditions [1]. The objective of this thesis work was to design one part of a system that allows driving the LEDs with fixed average currents with a variable DC voltage source without using voltage regulated LED driver ICs. The Pulse Width Modulation (PWM) approach was utilized in this thesis work. Figure 1 illustrates the block diagram of the LED card.

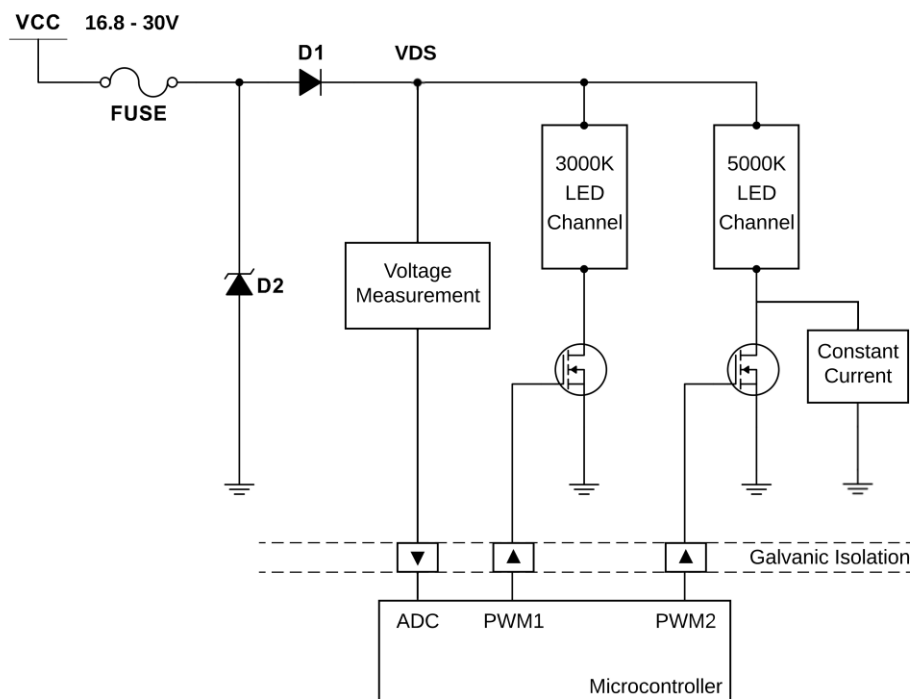


Figure 1. The block diagram of the LED card

The company has a subcircuit that is used to control the brightness of the LED card. The subcircuit is separated from the rest of the LED card circuit with galvanic isolation. The subcircuit includes a microcontroller like in figure 1 that has Analog to Digital Converter (ADC) inputs and PWM outputs. The LED card includes 3000K and 5000K color temperature LED channels. Each LED channel is divided into LED branches in parallel, and each branch consists of multiple LEDs in series. The LED branches are connected via Metal Oxide Semiconductor Field Effect Transistor (MOSFET) switches from the power supply to the ground. The N-channel MOSFETs are used. The gate voltages of the MOSFET switches are controlled by the corresponding LED channel's optocoupler. In this switch mode, currents through the LED branches are proportional to the supplied voltage: the higher the supply voltage, the higher the current. If the gate voltage of a MOSFET is connected to a PWM source, then the LED current is on and off according to the PWM signal. It means that the average LED current can be controlled with an appropriate PWM duty cycle even at a high peak LED current. For example, with randomly selected values, assume LED current is 10mA at 10V supply voltage at 100% PWM duty cycle, and at 15V supply voltage, LED current is 15mA at 100% PWM duty cycle. If the target LED current is 10mA, then the average current can be regulated to 10mA with a lower PWM duty cycle. It essentially states that when the supplied voltage is higher, the LED branch current can be controlled to the target average current with the appropriate PWM duty cycle. It requires 100% PWM duty cycle at 10V, it may require 50% PWM duty cycle at 15V, it may require 30% PWM duty cycle at 17V, and so on to maintain the average LED branch current to 10mA. The voltage level information of the DC voltage source is vital in this switch mode operation. So, the goal was that a circuit measures the input voltage of the LED card, and the measured voltage information is passed through the isolation barrier to the microcontroller. The microcontroller then decides the appropriate PWM duty cycle for the target brightness level, the PWM signals are passed through optocouplers to drive the LED channels, and the target average LED branch current is maintained in a limited power supply voltage range.

The 3000K and 5000K color temperature white LEDs were used for the LED card. The dimensions of the LED card are 500mm x 31mm consisting of 36 LEDs per color temperature. The LED cards are powered by a nominally 24V DC voltage source; however, the voltage varies between 16.8V and 30V.

The average current through the LED branches is 65mA at maximum brightness. The LED card is dimmable. LED channels are driven by 3kHz PWM signals. The LED card has an emergency path for the 5000K LED channel when the PWM signal for the 5000K LED channel is missing from the microcontroller. The 5000K LED branches continue operating at 20% current during this event.

The software department of the company is in charge of developing the program for the microcontroller based on this thesis work outcome.

2 Theoretical Background

This chapter includes a discussion of the theoretical backgrounds that aid in understanding the circuits presented in chapter 3.

2.1 Isolation

In electronics, galvanic isolation is accomplished by keeping proper clearance among the circuits and keeping the grounds of these circuits separated from each other. These different circuits may depend on each other for carrying out specific tasks. The isolation blocks current entering from one circuit to another circuit, prevents hazardous voltages appearing from one circuit to another circuit, improves noise immunity, helps prevent electrical shocks. [2.]

The benefit of isolation can be mentioned in the case of the LED card used in this thesis work. A controller interacts with the subcircuit to control the LED card, and the subcircuit is isolated from the main circuit. The microcontroller has vital roles in the subcircuit, and microcontrollers are generally powered by $\leq 5V$

DC voltage source. When the LED cards are exposed to transient voltages, the microcontrollers may get damaged, signals may get corrupted, eventually causing problems for the controller. Isolation safeguards the controller from such events.

There are isolator ICs commonly based on capacitive, magnetic, and optical coupling used for signal passing. Optical based isolators are called optocouplers. There are different types of optocouplers, such as optocouplers with phototransistor output, photodarlington output, linear optocouplers, high speed optocouplers, etc. Optocoupler with phototransistor output is discussed as this type was used in the LED card.

The optocoupler with phototransistor output can be called the standard optocoupler which is equipped with an LED on the input side and a phototransistor on the output side. The wavelength of the LED light ranges from red to infrared [3]. Figure 2 shows the diagram of a standard optocoupler.

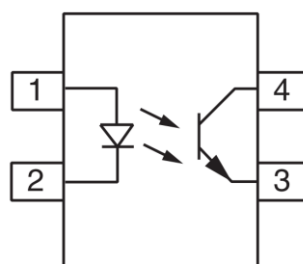


Figure 2. The diagram of an optocoupler with phototransistor output (Reprinted from [4])

The input side produces infrared light, and this light strikes the base of the phototransistor that generates current flow from the collector to the emitter of the phototransistor. The relationship between the currents through the LED and the collector-emitter is known as the Current Transfer Ratio (CTR). The relationship is expressed as [5,1]:

$$CTR = \frac{I_c}{I_f} \times 100\% \quad (1)$$

Here, I_c = Collector current
 I_f = LED current

The CTR is expressed as percentage. However, the CTR is not a constant parameter. Ambient temperature, LED current, collector-emitter voltage affect the CTR value. For example, the CTR value of TCMT1103 ranges from 100–200% [6,1]. The CTR also degrades over time due to heat stress on LED crystalline structure [7,2]. Two test results of CTR degradation published by Würth Elektronik [8] are shown in figure 3.

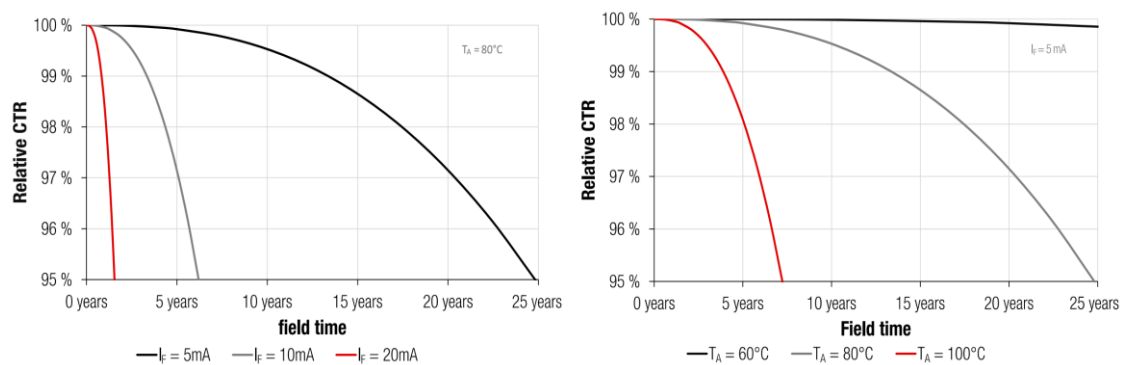


Figure 3. CTR degradation test result conducted by Würth Elektronik (Reprinted from [8])

The left side graph in figure 3 shows that the test was performed at three current levels through the LED, and the right side graph shows that the test was performed at different ambient temperatures at the same current. The graphs indicate that CTR degradation can be minimized by driving the LED with lower currents and using the optocoupler at lower ambient temperatures.

The CTR variation emphasizes that some considerations need to be taken so that the collector current does not fall below the minimum current required for an application. Manufacturers may include normalized CTR graphs to approximate the collector current. Figure 4 shows a normalized CTR graph of TCMT110 series optocouplers.

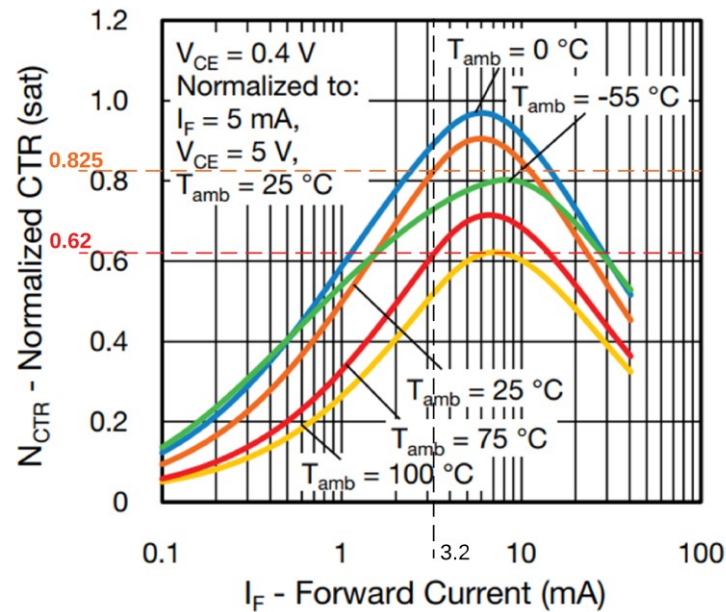


Figure 4. Normalized CTR values of TCMT110 series optocouplers at saturation (Modified from [6,6])

The CTR values are normalized to normal operating conditions, for example, at 5mA LED current, 25°C ambient temperature, 0.4V and 5V collector-emitter saturated and non-saturated voltage respectively. It can be observed from figure 4 that normalized CTRs keep increasing with an increase in LED forward current up to a certain point and then start decreasing. Normalized CTRs decrease with higher temperatures. The minimum CTR can be approximated by [5,3]:

$$CTR_{min} = CTR_{DMIN} \times NCTR \times Aging \times Negative\ tolerance \quad (2)$$

Here, CTR_{DMIN} = Minimum CTR in datasheet

$NCTR$ = Normalized CTR

$Aging$ = Aging factor

$Tolerance$ = Positive or negative tolerance

One example of the CTR calculation can be mentioned for the TCMT1103 optocoupler. Assume LED current $I_F = 3.2\text{mA}$, 20% aging and 25% tolerance factors, and the optocoupler is operated at minimum 25°C. From the graph in figure 4, NCTR is approximately 0.62 at 75°C and 0.825 at 25°C.

Minimum CTR, $CTR_{min} = 100 \times 0.62 \times 0.8 \times 0.75 = 37.2\%$ at 75°C

The minimum CTR at 25°C excluding the aging and tolerance factors is
 $CTR_{min} = 100 \times 0.825 = 82.5\%$

It is essential to look at the switching time versus load resistance graph when the standard optocoupler is used in a switching application. Figure 5 shows an example of it from the TCMT110 series optocoupler datasheet.

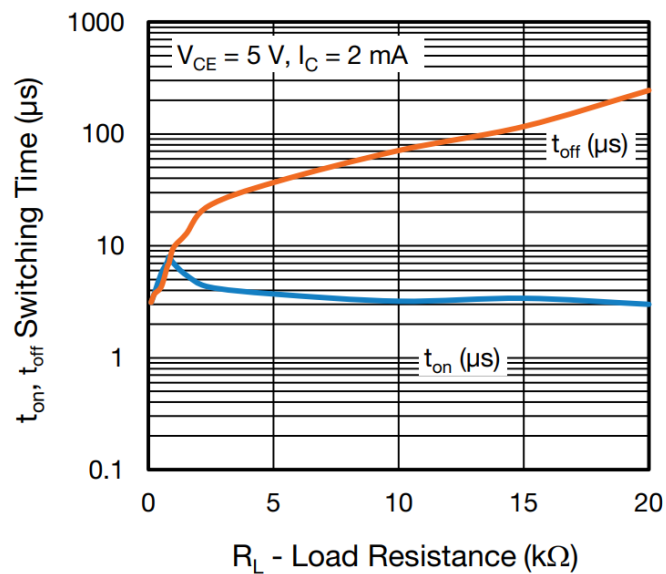


Figure 5. Switching time versus load resistance of TCMT110 series optocouplers (Reprinted from [6,6])

Figure 5 shows that switching time is dominated by phototransistor turn-off time mainly. Turn-off time increases with load resistance.

2.2 PWM Generation

One way to generate a PWM signal is by utilizing a sawtooth or triangular wave with a comparator. Basic sawtooth and triangular waveforms are shown in figure 6. The voltage rises linearly and then falls sharply or vice versa in a sawtooth waveform. On the other hand, voltage rise and fall times are generally equal in a triangular wave.

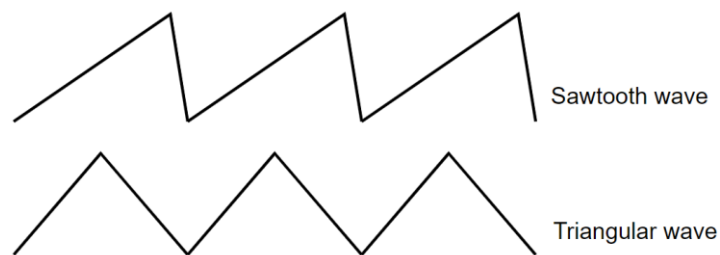


Figure 6. Sawtooth and triangular waveforms

A comparator compares an input voltage to a reference voltage and then outputs a voltage close to the positive supply or ground level in a single supply configuration; alternatively, the output can be stated to be high or low. The comparator output is high when the voltage at the non-inverting (+) terminal exceeds the inverting (-) terminal voltage. Contrarily, the comparator output is low when the inverting terminal voltage exceeds the non-inverting terminal voltage. Comparators mainly come with two output types: push-pull and open collector or open drain [9,6].

Assume the period of a triangular wave is $1000\mu\text{s}$, and it rises from 0V to 5V . The triangular wave source and a 1.5V reference voltage are connected to the non-inverting and inverting terminals of a comparator respectively. The comparator is powered by a 5V source where the negative voltage is 0V or ground. The comparator output is low as long as the triangular wave voltage is lower than 1.5V , as the inverting terminal is still higher than the non-inverting terminal. Then the comparator output becomes high when the triangular voltage exceeds the 1.5V reference. The output stays high until the triangular voltage

falls below 1.5V. The same event occurs when the triangular wave again exceeds the 1.5V reference, and the comparator eventually generates a square wave as long as the triangular wave continues and the 1.5V reference exists. The triangular wave frequency is fixed. By changing the reference voltage, the comparator can generate a PWM signal as the duty cycle changes with the change in the reference voltage. The generated PWM signal has an equal frequency as the triangular wave. The output waveform of the comparator is illustrated in figure 7.

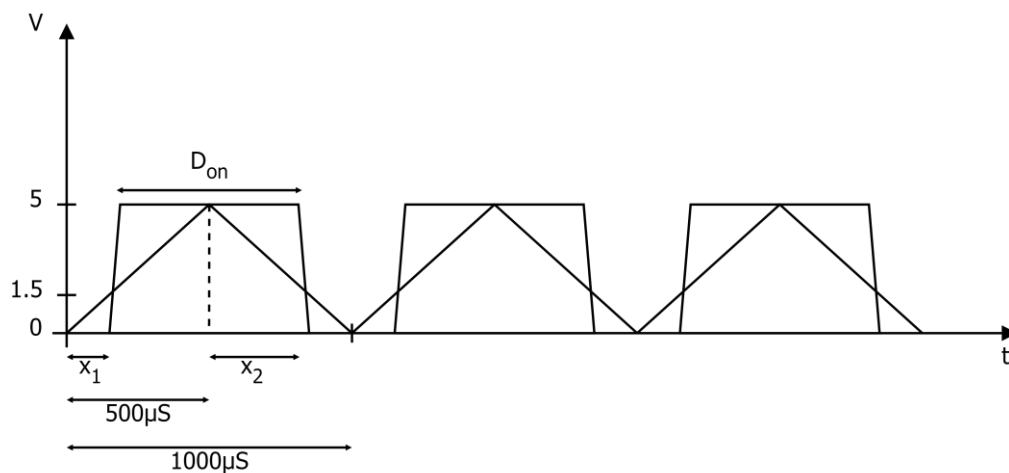


Figure 7. The comparator output

The duty cycle can be calculated as follows. The triangular wave rises from 0V to 5V linearly up to 500µs. The slope is, $m_1 = \frac{0-5}{0-500\mu s} = 10000$. Similarly, for 5V to 0V linear voltage fall of the triangular wave, the slope is, $m_2 = -10000$. It yields two equations.

$$y_1 = m_1 x_1; \text{ and } y_2 = m_2 x_2 + 5$$

Here, x and y refer to the time and voltage respectively, of the triangular wave. The on time of the PWM can be calculated from:

$$D_{on} = 500\mu s - x_1 + x_2 = 500\mu s - \frac{y_1}{m_1} + \frac{y_2 - 5}{m_2}$$

A $y_1 = y_2 = 1.5V$ reference voltage makes $D_{on} = 0.0007$ yielding $\frac{0.0007}{1000\mu S} \times 100 = 70\%$. Similarly, a 3V reference voltage yields a 40% duty cycle. The duty cycle is inversely proportional to the reference voltage in this example. The duty cycle would be proportional to the reference voltage if the reference voltage is connected to the non-inverting terminal and the triangular wave is connected to the inverting terminal of the comparator.

The duty cycle with a sawtooth wave can be approximated by ignoring linear voltage fall if the fall is very sharp. For the sawtooth wave replacing the triangular wave, $m = \frac{0-5}{0-1000\mu S} = 5000$; $D_{on} = 1000\mu S - \frac{y}{m}$

The duty cycle equations are presented in this section by assuming the ideal scenario, such as an instant high to low or low to high output transition of the comparator. However, there is a certain time associated with output transition, therefore, the equations can determine the duty cycle approximately.

2.3 PWM to DC Voltage

The DC component of a PWM signal is the average of the PWM signal. Figure 8 shows a timing diagram of a PWM signal.

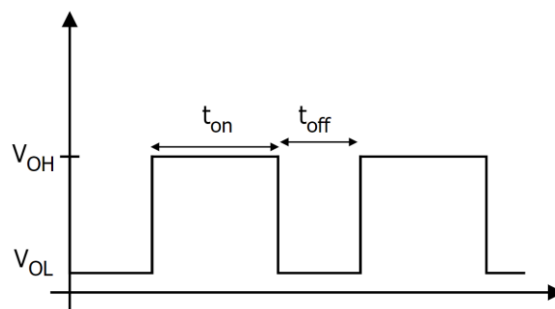


Figure 8. Timing diagram of a PWM signal

DC component of a PWM signal can be calculated as:

$$DC_{PWM} = \frac{t_{on}}{T} V_{OH} + \frac{t_{off}}{T} V_{OL}$$

$$DC_{PWM} = DV_{OH} + (1 - D)V_{OL} = DV_{OH} + V_{OL} - DV_{OL}$$

$$DC_{PWM} = (V_{OH} - V_{OL})D + V_{OL} \quad (3)$$

Here, DC_{PWM} = DC component of the PWM signal

D = Duty cycle ranging from 0 to 1

T = Period of the PWM

V_{OH} = High voltage level of the PWM

V_{OL} = Low voltage level of the PWM

DC component of a PWM signal can be retrieved by using a low pass filter with a cutoff frequency close to 0Hz. There are two options: passive low pass filter and active low pass filter. A first order passive RC low pass filter can be formed by figure 9 below.

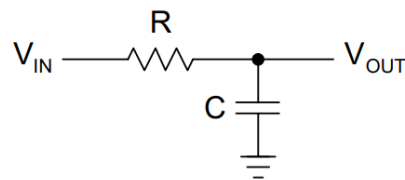


Figure 9. The first order RC low pass filter (Reprinted from [10,2])

The cutoff frequency (f_c) of this RC low pass filter is [10,2]:

$$f_c = \frac{1}{2\pi RC}$$

However, passive filters have impedance loading issues that can be avoided by active filters [11,7]. Active filters are realized using op-amps, resistors, and capacitors [10,1].

Low pass filters are often designed based on different filter characteristics, such as Butterworth, Chebyshev, and Bessel. Butterworth filters have maximally flat response in the passband with slight overshoot in step response. Chebyshev filters have ripple in the passband with overshoot in step response. Bessel filters have flat response in the passband and lesser overshoot than the

Butterworth filters in the step response. Bessel filters have slower attenuation rate than the Butterworth and Chebyshev filters in the transition region, while Chebyshev filters have the steepest slope among the three. Bessel filters have a better linear phase response than the other two in the passband. Low pass filter parameters are illustrated in figure 10 based on [13,3]. [12,3.]

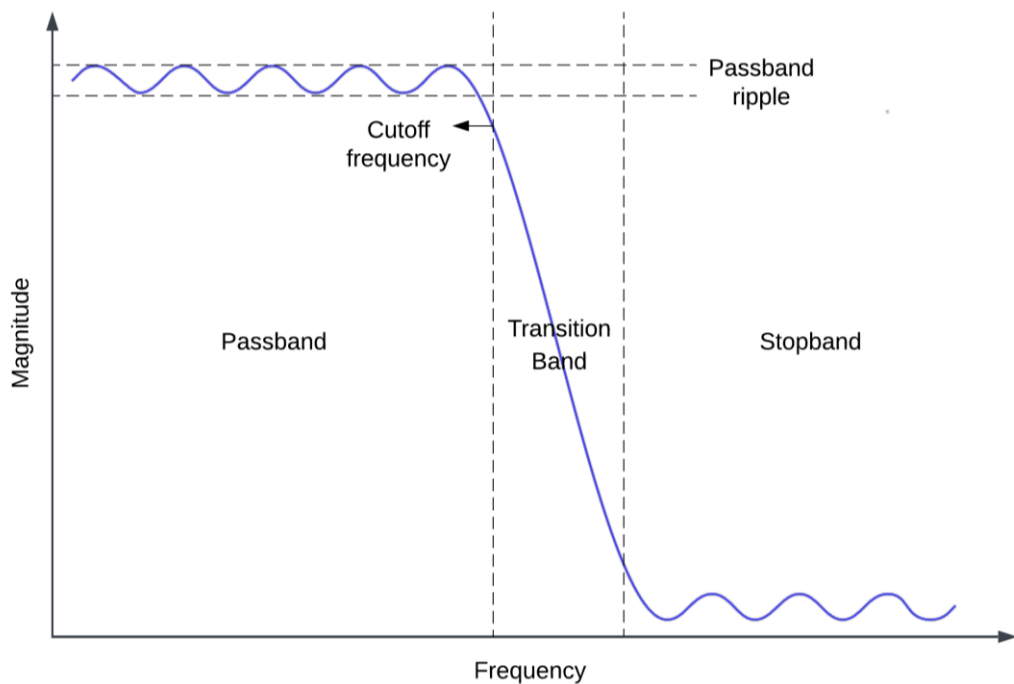


Figure 10. Low pass filter parameters

Comparative magnitude responses of these filters are shown in figure 11. The responses are from eight pole Butterworth, 0.5 dB ripple Chebyshev, and Bessel filters. The step response comparison is shown in figure 12. The filters have 1Hz cutoff frequency. [13,25.]

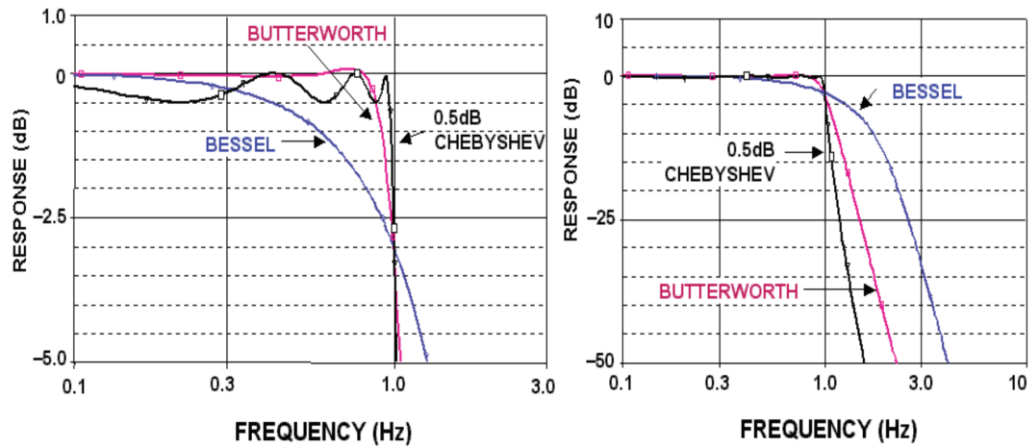


Figure 11. The magnitude response comparison for eight pole Butterworth, 0.5 dB ripple Chebyshev, and Bessel filters (Reprinted from [13,25])

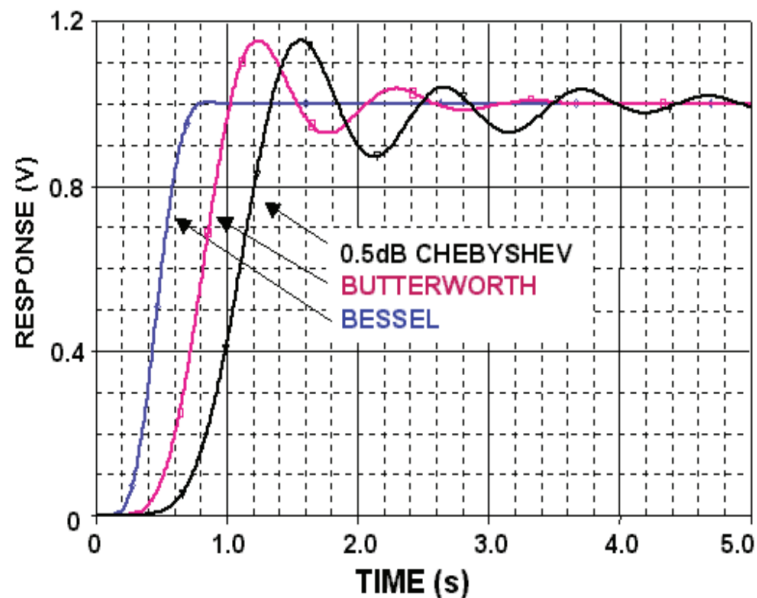


Figure 12. Step response comparison of the same filters shown in figure 11 (Reprinted from [13,25])

The step response shows that the Chebyshev filter takes the longest time to settle while the Bessel filter takes the shortest. Both Butterworth and Chebyshev filters have overshoot and ringing.

The transfer functions of first and second order filters are in equations (4) and (5) [10,11]. A_0 is passband gain at DC.

$$A(s) = \frac{A_0}{1+a_i s} \quad (4)$$

$$A_i(s) = \frac{A_0}{1+a_i s+b_i s^2} \quad (5)$$

A higher order number of filters can be realized by cascading the first and second order filters. For example, one first order filter and two second order filters can be cascaded to form a fifth order filter. a_i and b_i in equations (4) and (5) are the filter coefficients that form a particular filter characteristic. The filter coefficients can be found in filter coefficients tables [10,56-62]. A first order unity gain non-inverting active low pass filter can be realized by the circuit in figure 13.

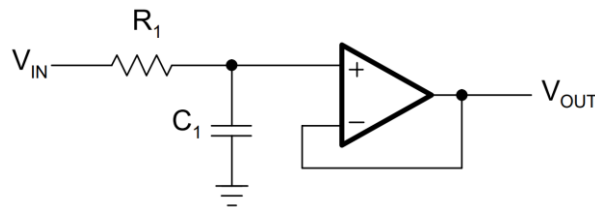


Figure 13. Unity gain first order non-inverting active low pass filter (Reprinted from [10,14])

The transfer function of this first order filter is [10,13]):

$$A(s) = \frac{1}{1+2\pi f_c R_1 C_1 s} \quad (6)$$

By comparing the transfer function at equation (6) to the general first order low pass filter transfer function at equation (4), the following relationships can be derived [10,13]):

$$A_0 = 1; a_i = 2\pi f_c R_1 C_1; R_1 = \frac{a_i}{2\pi f_c C_1}$$

A second order active low pass filter can be realized by Sallen-Key and Multiple Feedback topologies. The multiple feedback topology offers better high

frequency behavior, and Sallen-Key offers better gain response in the passband. The design equations for Sallen-Key topology are presented below. [12,3.]

A second order unity gain Sallen-Key low pass filter circuit is shown in figure 14.

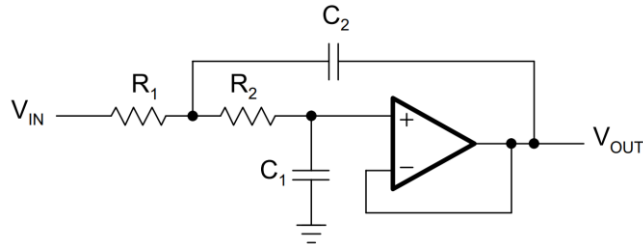


Figure 14. The second order unity gain Sallen-Key low pass filter (Reprinted from [10,15])

The transfer function of this Sallen-Key low pass filter is [10,15]:

$$A(s) = \frac{1}{1 + 2\pi f_c C_1 (R_1 + R_2) s + (2\pi f_c)^2 R_1 R_2 C_1 C_2 s^2}$$

By comparing the Sallen-Key unity gain transfer function to equation (5), the following relationships can be formed [10,15-16]:

$$A_0 = 1; a_i = 2\pi f_c C_1 (R_1 + R_2); b_i = (2\pi f_c)^2 R_1 R_2 C_1 C_2$$

$$R_1 = \frac{a_i C_2 - \sqrt{a_i^2 C_2^2 - 4b_i C_1 C_2}}{4\pi f_c C_1 C_2}; R_2 = \frac{a_i C_2 + \sqrt{a_i^2 C_2^2 - 4b_i C_1 C_2}}{4\pi f_c C_1 C_2}$$

The capacitors must fulfill the following condition:

$$C_2 \geq C_1 \frac{4b_i}{a_i^2}$$

The pole frequency of the Sallen-Key low pass filter can be found by [14,4]:

$$f_c = \frac{1}{2\pi\sqrt{R_1R_2C_1C_2}} \quad (7)$$

In Sallen-Key low pass filter topology, the magnitude response may show an upward trend at a frequency above the cutoff frequency. The addition of an RC low pass filter at the output of the Sallen-Key low pass filter helps solve this issue. A comparative example is shown in figure 15, where it shows the magnitude responses of a 1kHz Sallen-Key low pass filter with and without an RC low pass filter. This RC filter places a pole at about 40kHz, which improves the high frequency response. [12,16.]

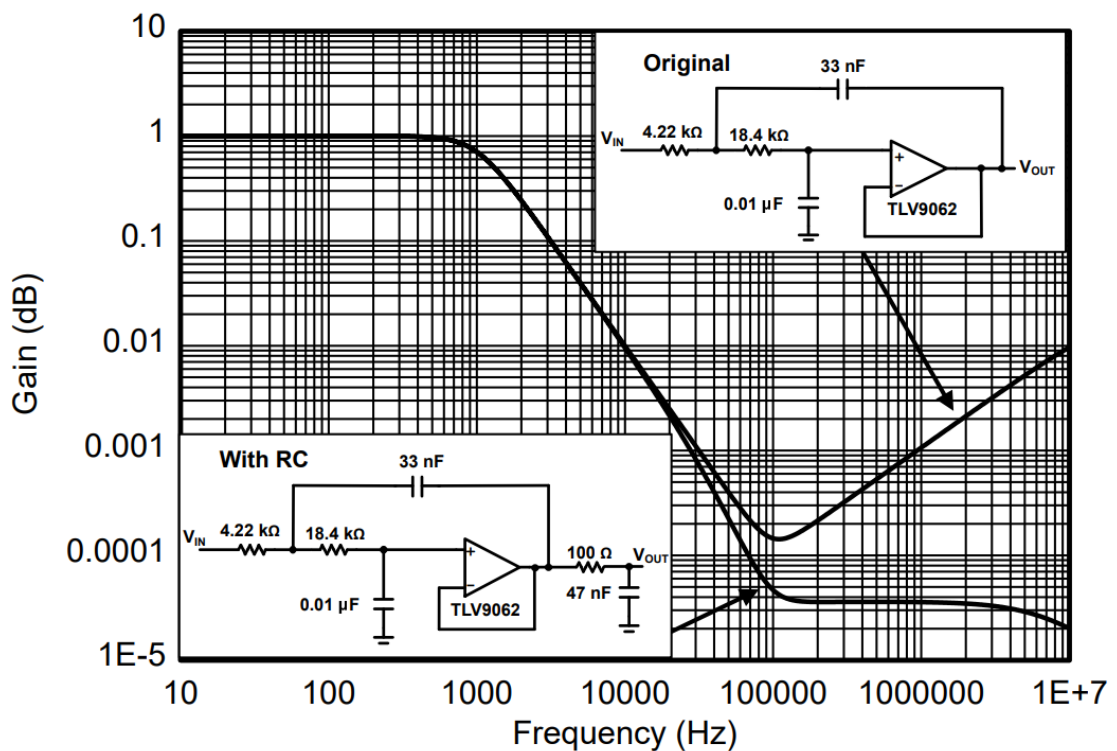


Figure 15. A comparison of magnitude responses of a Sallen-Key low pass filter with and without an RC filter (Reprinted from [12,16])

There are also online filter calculators that can be utilized in filter designing. For example, Analog Devices [15], Texas Instruments [16], OKAWA Electric Design [17] provide such calculators.

2.4 Op-amp Circuits

An op-amp has high input and low output impedances. These characteristics can be utilized to make an operational amplifier (op-amp) buffer circuit. There are common situations that a source cannot supply enough current to a low impedance load, eventually the source is loaded. Op-amp buffer circuits can be essential in such cases. Examples could include the analog measurement with the ADC of a microcontroller, voltage reference from a voltage divider, etc. A unity gain op-amp buffer circuit is shown in figure 16. The output voltage V_o is ideally equal to the input voltage V_i . [18.]

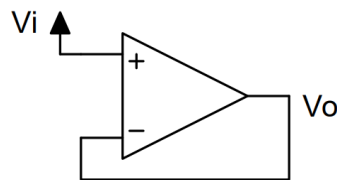


Figure 16. Op-amp buffer circuit [18]

An op-amp is also used to compare a signal to a reference voltage to output an error voltage. An inverting op-amp with a positive reference voltage in a single supply configuration is shown in figure 17.

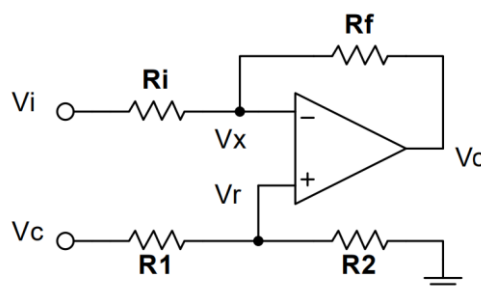


Figure 17. Op-amp difference amplifier

In figure 17, the voltage reference V_r can be taken from a voltage divider formed by R_1 and R_2 resistors.
$$V_r = \frac{R_2}{R_1 + R_2} V_c$$

The input signal is connected to the open end of the R_i resistor. As input terminals of the Op-amp are almost equal due to the negative feedback, $V_r = V_x$

Assume the current flows from the left to the right side. Then $\frac{V_i - V_x}{R_i} = \frac{V_x - V_o}{R_f}$

$$\frac{V_o}{R_f} = \frac{V_x}{R_f} - \frac{V_i - V_x}{R_i}; \Rightarrow V_o = V_x - \frac{(V_i - V_x)R_f}{R_i}$$

$$V_o = V_r - \frac{(V_i - V_r)R_f}{R_i} \quad (8)$$

The addition of a capacitor across the feedback resistor R_f helps the circuit in figure 17 with stability, and the cutoff frequency is [19,4]:

$$f_c = \frac{1}{2\pi R_f C} \quad (9)$$

2.5 TL431

TL431 is a versatile IC that is used in many applications. TL431 contains an internal 2.5V reference voltage and an op-amp. Figure 18 shows the equivalent circuit of TL431.

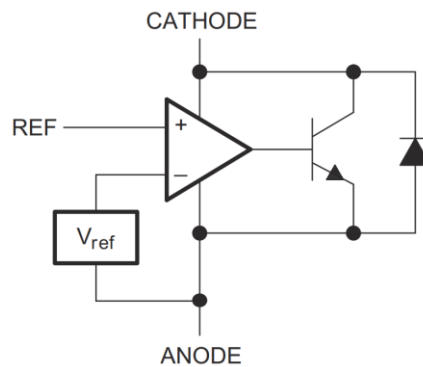


Figure 18. The equivalent circuit of TL431 (Reprinted from [20,20])

TL431 can work as an adjustable voltage reference from 2.5V to 36V at the cathode terminal [20,20]. An adjustable voltage reference circuit is shown in figure 19.

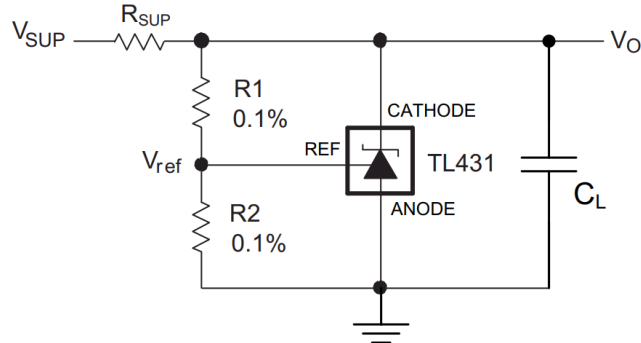


Figure 19. TL431 adjustable voltage reference circuit (Reprinted from [20,25])

The output voltage V_o can be calculated by the following equation [20,25]:

$$V_o = \left(1 + \frac{R_1}{R_2}\right) V_{REF} - I_{REF} R_1 \quad (10)$$

Here, $V_{REF} = 2.5V$; I_{REF} = Current through reference terminal (2–4 μA) [20,6].

2.6 LED Circuits

LEDs can be driven in constant current (CC) and switch modes. Some basic constant current circuits and the switch mode circuit are discussed in this section.

2.6.1 Single Transistor Based CC

An NPN bipolar junction transistor operates in three regions: active, saturation, and cutoff. Ideally, there is no current flow from the collector to the emitter when the NPN transistor is in the cutoff region. The cutoff region is achieved by reverse biasing the base-emitter junction. The collector current I_C is approximately constant in the varying collector-emitter voltage V_{CE} at lower

base-emitter V_{BE} voltages as in figure 20. The active region can be achieved by forward biasing the base-emitter junction and reverse biasing the base-collector junction. The NPN transistor enters the saturation region when both base-collector and base-emitter junctions are forward biased. [21,307.]

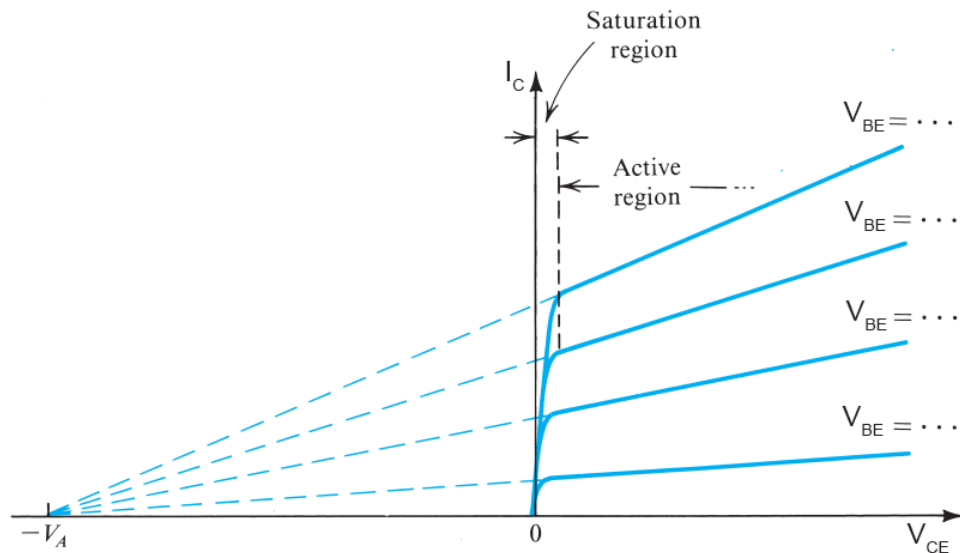


Figure 20. The collector current of an NPN transistor at different V_{BE} voltage levels (Modified from [21,327])

The voltage at the collector should be higher than the base terminal to stay in the active region. However, the PN junction starts to conduct beyond approximately 0.4V; therefore, the collector voltage may go below 0.4V than the base voltage to maintain the active region, and going further below the NPN transistors starts to enter the saturation region [21,316].

The LEDs can be driven in CC mode by operating an NPN transistor in the active region. The circuit is shown in figure 21 based on the AN90026 application note from Nexperia [22].

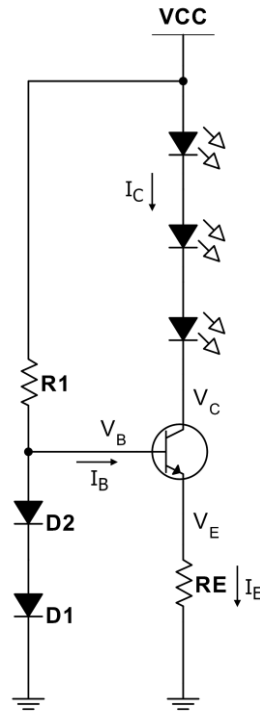


Figure 21. Single transistor based constant current circuit

In the active region, the following equations stand [21,309]:

$$I_C = \beta I_B; I_B = \frac{I_C}{\beta}; I_E = I_C + I_B; I_E = \frac{V_E}{R_E}$$

Here, $I_C =$ Collector current

$I_B =$ Base current

$I_E =$ Emitter current

$\beta =$ Current gain

The base is at two diode voltage drop of approximately 1.4V, and the base-emitter voltage drop is approximately 0.7V. It makes the emitter voltage, $V_E = V_B - V_{BE} = 1.4 - 0.7 = 0.7V$. The change of a few volts in VCC causes a change at V_B in millivolt range. Therefore, the emitter voltage V_E changes little so does the emitter current. The resistor value R_1 should be calculated using the minimum current gain β in the datasheet of the transistor. The current gain β may range from 50 to 200 or even achieve higher values [21,309], which makes

the consideration of $I_C \approx I_E$ in many applications. The total voltage drop over all LEDs should be such that the collector voltage V_C is above the base voltage V_B . With such conditions, this circuit can regulate approximately constant current through the LEDs within a certain VCC limit.

2.6.2 Two Transistors Based CC

Two NPN transistors are used in this circuit in a feedback loop. The circuit is shown in figure 22 based on [23].

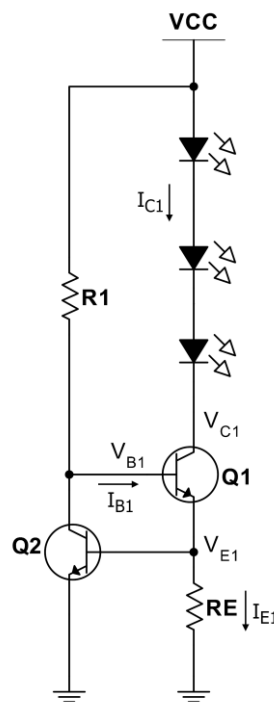


Figure 22. Two NPN transistors based constant current circuit

The base of the Q2 NPN transistor is connected to the emitter terminal of the Q1 NPN transistor. Assume the base-emitter voltage drop for both Q1 and Q2 transistors is 0.7V, and the Q2 transistor is off at first. The current starts flowing through the Q1 transistor, and this develops a voltage drop over R_E . When this voltage starts to exceed 0.7V, the Q2 transistor starts to conduct which reduces Q1 transistor base voltage V_{B1} and current I_{B1} . This results in reduced collector current I_{C1} , so the voltage across R_E starts to reduce to 0.7V. When V_{E1} goes

lower than 0.7V, the Q2 transistor starts to turn off. This loop continues to regulate 0.7V at the emitter of Q1 or base of Q2, and it regulates a constant current through the LEDs. The emitter I_{E1} current can be calculated as:

$$I_{E1} = \frac{V_{BE2}}{R_E}; \quad V_{BE2} = \text{Base-emitter drop of Q2 transistor.}$$

2.6.3 Op-amp and Transistor Based CC

An op-amp and an NPN transistor form the circuit shown in figure 23 based on [23].

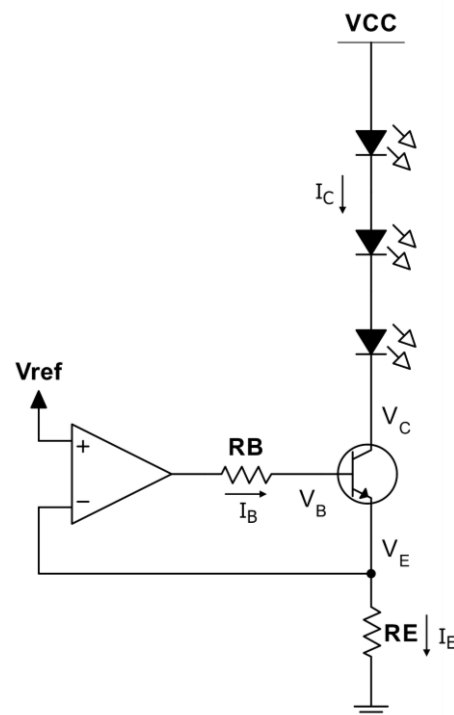


Figure 23. Op-amp and NPN transistor based constant current circuit

The base of the transistor is connected to the op-amp output through an R_B resistor. The non-inverting terminal of the op-amp is connected to the voltage reference V_{ref} , and the feedback is taken from the emitter of the transistor. Voltages at the inverting and non-inverting terminals are almost equal when the op-amp is operated in negative feedback. Therefore, $V_E \approx V_{ref}$. The op-amp strives to maintain this relationship by supplying adequate current to the base of the transistor; therefore, the LED current is approximately, $I_C = \frac{V_{ref}}{R_E}$

2.6.4 Switch Mode

An N-channel MOSFET has three operating regions: triode, cutoff, and saturation region. The MOSFET turns on and creates a conducting channel between the drain and source when the gate to source voltage V_{GS} equals the threshold voltage V_{TH} [21,251]. The charge in the channel increases with higher V_{GS} , allowing more current to flow from the drain to the source. The switching application is implemented by operating the MOSFET in the triode region. Triode region can be achieved by making $V_{DS} < V_{GS} - V_{TH}$, here V_{DS} is drain to source voltage [21,266]. The MOSFET starts entering the cutoff region with $V_{GS} < V_{TH}$.

LEDs can be driven in switch mode with an MOSFET switch to control the average current through the LEDs. The circuit is shown in figure 24.

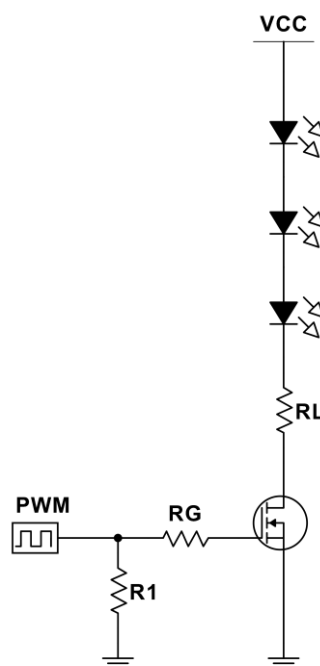


Figure 24. LED control with N-channel MOSFET switch

The LEDs are connected from the supply voltage V_{CC} to the drain of the MOSFET through an R_L current limiting resistor. The gate of the MOSFET is

controlled by a PWM source, and there is an R_G resistor in between. The current through the LEDs can be approximated by:

$$I_{max} = \frac{VCC - nV_f}{R_L + R_{DS(on)}} \quad (11)$$

$$R_L = \frac{VCC - nV_f}{I_{max}} - R_{DS(on)} \quad (12)$$

Here, VCC = Voltage supply
 n = Number of LEDs
 V_f = LED forward voltage
 R_L = Series resistor
 $R_{DS(on)}$ = MOSFET's drain to source resistance
 I_{max} = LED current when the MOSFET is on

However, LEDs follow a diode behaviour, meaning the voltage across an LED and the current through the LED do not hold a linear relationship. An example of an I-V curve of a white LED is shown in figure 25.

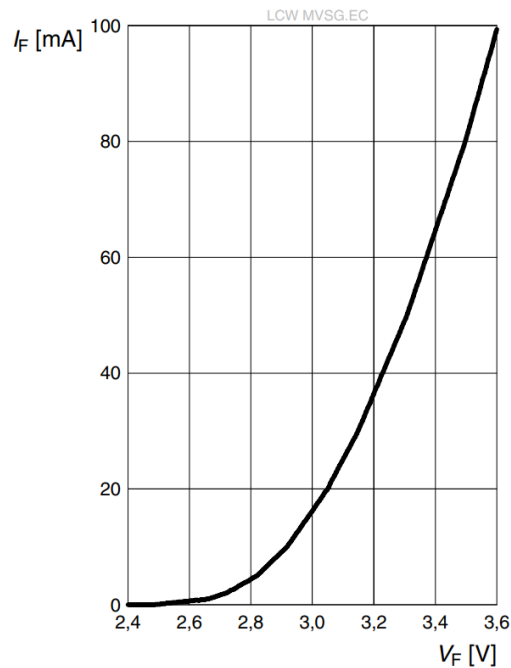


Figure 25. An example of a white LED I-V curve (Reprinted from [24])

As it can be seen from figure 25, the I-V curve is exponential. The LED forward voltage V_f should be determined from the I-V curve in the LED datasheet at the corresponding LED forward current or by measurement when using equations (11) and (12).

The gate of the MOSFET forms a capacitor that needs to be charged to reach V_{GS} . R_G is used to limit the inrush current, and the R_1 resistor is used to discharge the gate voltage when the MOSFET should be off. The MOSFET might not turn off if there is no discharge path for gate capacitor charges.

By connecting a PWM signal between R_G and R_1 , the MOSFET can be switched on and off causing the LED current on and off, and this makes an average current through the LED. The average current I_{avg} can be calculated by the PWM duty cycle D and the LED current I_{max} at on time:

$$I_{avg} = DI_{max} \quad (13)$$

3 Circuits Description

The circuit diagram has been shown in figure 1. The LED card is protected against high voltage with a nominally D2 35.1V transient voltage suppressor diode that has a maximum clamping voltage of 48.4V and reverse polarity voltage with D1 0.71V diode. The description of the circuit is divided into two parts: isolated DC voltage measurement and LED circuits. Both voltage measurement and LED circuits are powered from the VDS net, as shown in figure 1. These two parts are discussed in this chapter.

3.1 Isolated DC Voltage Measurement Circuits

The CTR of a standard optocoupler is not static, as seen in section 2.1. The selection of the correct CTR value becomes challenging if the CTR value appears on the voltage measurement equation. Linear optocoupler and isolation amplifier ICs could replace the standard optocouplers in the voltage

measurement circuit. However, linear optocoupler and isolation amplifier ICs were expensive to be used in this thesis work application. The company required the voltage measurement circuit with the standard optocouplers only and to use the ADC of the microcontroller in the subcircuit for the measurement.

It is essential to convert the power supply voltage information into some other form that could be passed through the standard optocoupler to the measurement side without significant dependence on the CTR and form voltage measurement equations where the CTR parameter does not appear. This approach would produce more accurate measurements when the standard optocouplers are used.

A PWM based technique for the voltage measurement was developed in this thesis work. The power supply voltage information is converted into a PWM signal, the PWM signal is transferred across the isolation, then the PWM signal is converted back to the analog voltage, and the microcontroller measures it. However, it was presumed by the company that PWM based voltage measurement circuit would interfere with other signals; therefore, the company decided to continue with a TL431 based voltage measurement circuit. Isolation amplifier and linear optocoupler based voltage measurement circuits were also built on breadboards quickly to see their performances.

3.1.1 Linear Optocoupler Based Voltage Measurement

Linear optocouplers are built with an LED and closely matched two photodiodes. The photodiode currents are generally linearly related to the LED current, and the photocurrents through both photodiodes are nominally equal [25,4]. A linear optocoupler can be put into a servo feedback loop that eliminates the dependency on LED current [25,4]. There are linear optocouplers such as IL300, HCNR201, etc. The circuit shown in figure 26 is configured into

photovoltaic mode based on the IL300 application note [25,5].

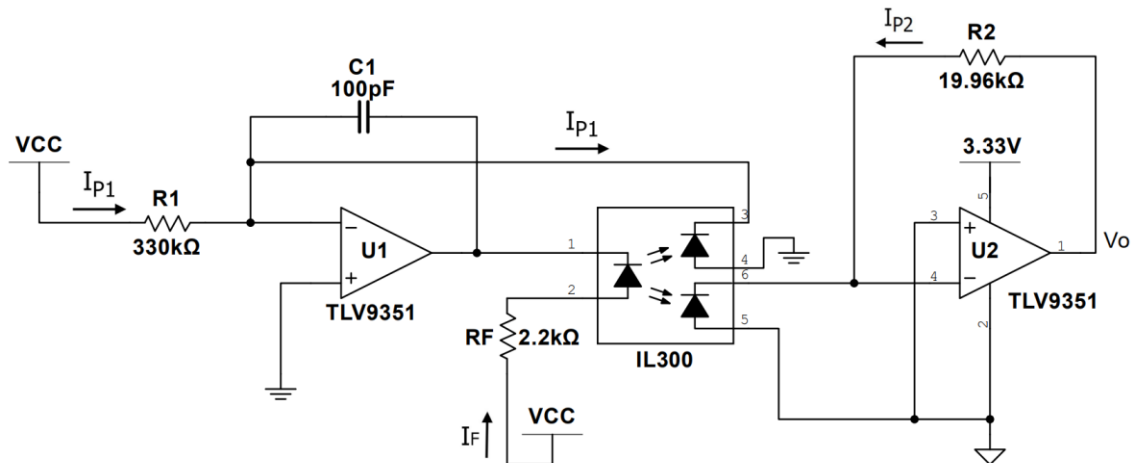


Figure 26. Linear optocoupler based voltage measurement circuit

The input signal is taken from VCC, and the output signal is measured from the output of the U2 op-amp. TLV9351 was used for both U1 and U2 op-amps. U1 was powered by VCC, and a 3.33V source powered up U2 op-amp on the measurement side. Inverting and non-inverting terminals of U1 are essentially at zero volt due to the loop. Photodiode current I_{P1} depends on the R_1 resistor and equals to $\frac{V_{CC}}{R_1}$. Equal photodiode current I_{P2} flows through the R_2 resistor. The following equations are based on the application note [25,2-5]. The transfer function of this circuit is $\frac{V_o}{V_{CC}} = \frac{K_3 \times R_2}{R_1}$. The transfer gain, $K_3 = \frac{K_2}{K_1}$. Here, $K_1 = \frac{I_{P1}}{I_F}$ and $K_2 = \frac{I_{P2}}{I_F}$; I_F is LED current. As K_3 is targeted to be 1, $\frac{V_o}{V_{CC}} = \frac{R_2}{R_1}$ and

$$V_{CC} = \frac{V_o R_1}{R_2} \quad (14)$$

On the breadboard measurement, it was found that non-zero voltage appears at the inverting terminal of U1 op-amp with R_1 less than approximately 330kΩ at VCC ranging from 16V to 30V. $R_1=330\text{k}\Omega$ and $R_2=19.96\text{ k}\Omega$ were used.

3.1.2 Isolation Amplifier Based Voltage Measurement

There are isolation amplifier ICs like AMC1311B that can be used for isolated voltage measurement. AMC1311B is based on capacitive isolation that can measure -0.1V to 2V within its specifications [26,22]. The input stage converts the analog voltage into a digital bitstream that is passed through the isolation [26,20]. The output stage converts the bitstream into a differential signal with unity gain [26,20;26,22]. The input side supports a 4.5V to 5.5V power supply, and the output side supports a 3V to 5.5V power supply [26,6]. The circuit shown in figure 27 is based on the AMC1311B application note [26,25].

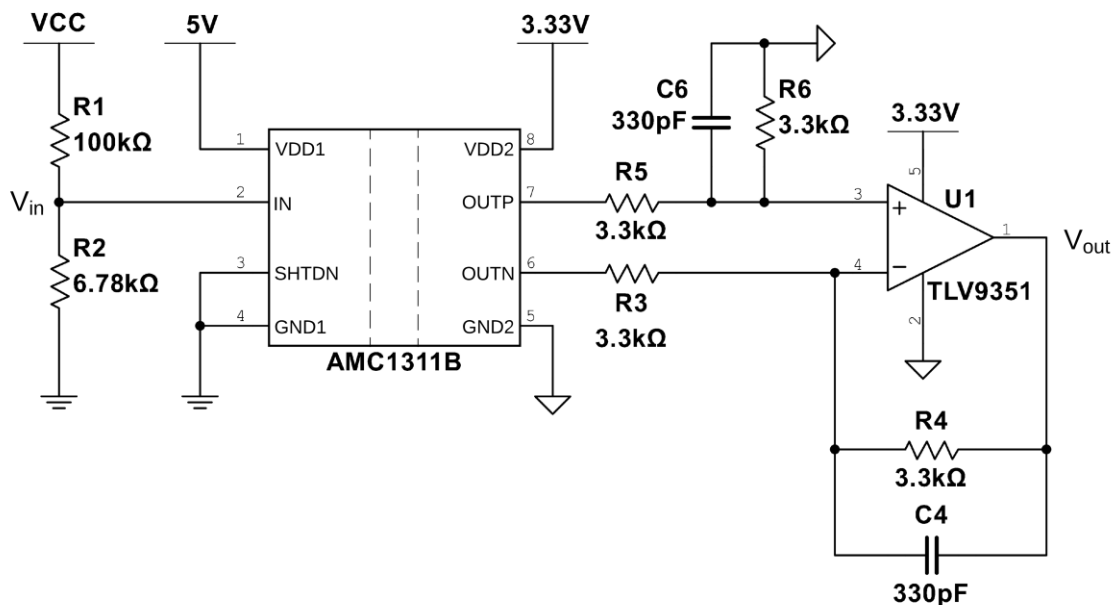


Figure 27. AMC1311B based voltage measurement circuit

The input section of AMC1311B was powered by 5V, and the output section was powered by 3.3V. VCC voltage was scaled down to the effective range with the voltage divider formed by R₁ and R₂ at pin 2 of AMC1311B. V_{in} ranges from $\frac{16V \times R_2}{R_2 + R_1} = \frac{16V \times 6.78k\Omega}{6.78k\Omega + 100k\Omega} = 1.016V$ to $\frac{30V \times 6.78k\Omega}{6.78k\Omega + 100k\Omega} = 1.9V$ from 16V to 30V VCC. The voltage difference between OUTP and OUTN pins is equal to the input voltage V_{in}. A difference amplifier formed by U1 TLV9351 was used to subtract OUTN voltage from OUTP with unity gain by selecting R₃ = R₄ = R₅ = R₆ = 3.3kΩ

and $C_4 = C_6 = 330\text{pF}$ as per the application note [26,25]. As $V_{out} = V_{in}$, V_{out} can be converted back to V_{CC} by:

$$V_{CC} = \frac{V_{out}(R_1 + R_2)}{R_2} \quad (15)$$

3.1.3 TL431 Based Voltage Measurement

This voltage measurement circuit is based on TL431. The circuit is shown in figure 28.

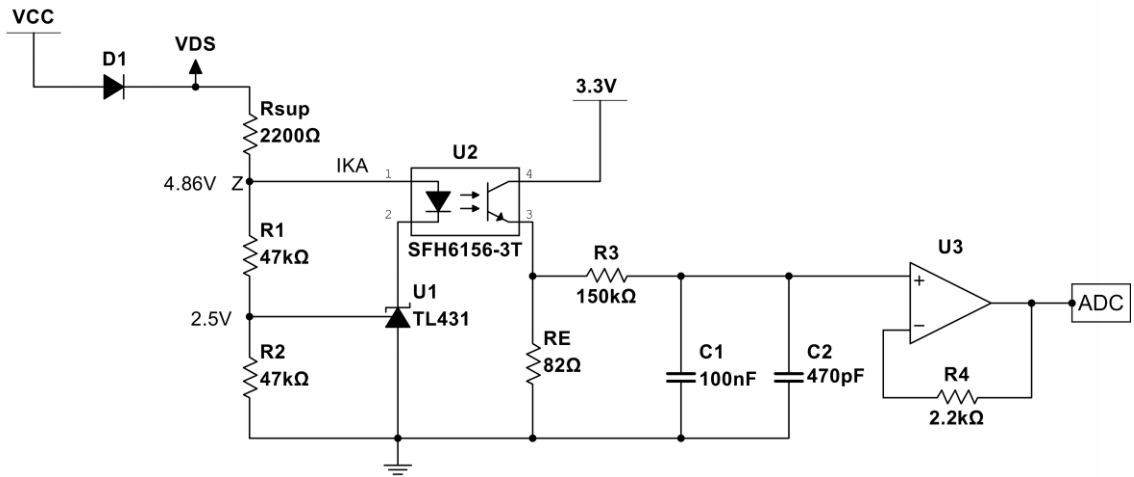


Figure 28. TL431 based voltage measurement circuit

The LED of SFH6156-3T optocoupler is placed in the path of shunt regulation, as shown in section 2.5. $R_1 = R_2 = 47\text{k}\Omega$ makes approximately 4.86V at point Z by equation (10) between 16.8V and 30V power supply:

$$V_Z = \left(1 + \frac{47\text{k}\Omega}{47\text{k}\Omega}\right) 2.5 - 3\mu\text{A} \times 47\text{k}\Omega = 4.86\text{V}$$

The current drawn by R_{SUP} from V_{DS} net is divided into optocoupler LED current I_{KA} and R_1 current. Assuming 0.71V voltage drop across the D_1 diode,

$$\frac{V_{CC} - 0.71 - V_Z}{R_{SUP}} = I_{KA} + \frac{V_Z - 2.5\text{V}}{R_1}$$

$$I_{KA} = \frac{V_{CC} - 0.71 - V_Z}{R_{SUP}} - \frac{V_Z - 2.5V}{R_1} \quad (16)$$

$$V_{CC} = \left(I_{KA} + \frac{V_Z - 2.5V}{R_1} \right) R_{SUP} + V_Z + 0.71 \quad (17)$$

$$\text{At 16.8V power supply, } I_{KA} = \frac{16.8V - 0.71V - 4.86}{2.2k\Omega} - \frac{4.86 - 2.5V}{47k\Omega} = 5.05mA$$

$$\text{At 30V power supply, } I_{KA} = \frac{30V - 0.71V - 4.86}{2.2k\Omega} - \frac{4.86 - 2.5V}{47k\Omega} = 11.05mA$$

The collector of the optocoupler's transistor was connected to 3.3V. The emitter voltage is buffered by the U3 op-amp. There is an RC low pass filter between the optocoupler's emitter voltage and U3 buffer formed by $R_3=150k\Omega$, $C_1=100nF$, and $C_2=470pF$. The ADC of the microcontroller measures the output of the U3 buffer. Optocoupler's CTR graph is not present in the datasheet. CTR values were measured on the LED card PCBs. These values are presented in tables 3 and 4 in the result section.

3.1.4 PWM Based Voltage Measurement

As shown in section 2.2, an analog voltage can be converted into a PWM signal using a comparator and a sawtooth or triangular wave. The duty cycle varies with the input voltage level that is fed to the comparator. It was searched on the internet what type of ICs available that have the components to convert an analog voltage into a PWM signal, support 16.8V–30V supply voltage, and are inexpensive enough to meet the company's budget for the voltage measurement circuit. TL494 PWM controller IC meets the supply voltage range, includes all the components for the purpose, and is one of the cheapest options. The functional block diagram of TL494 is shown in figure 29.

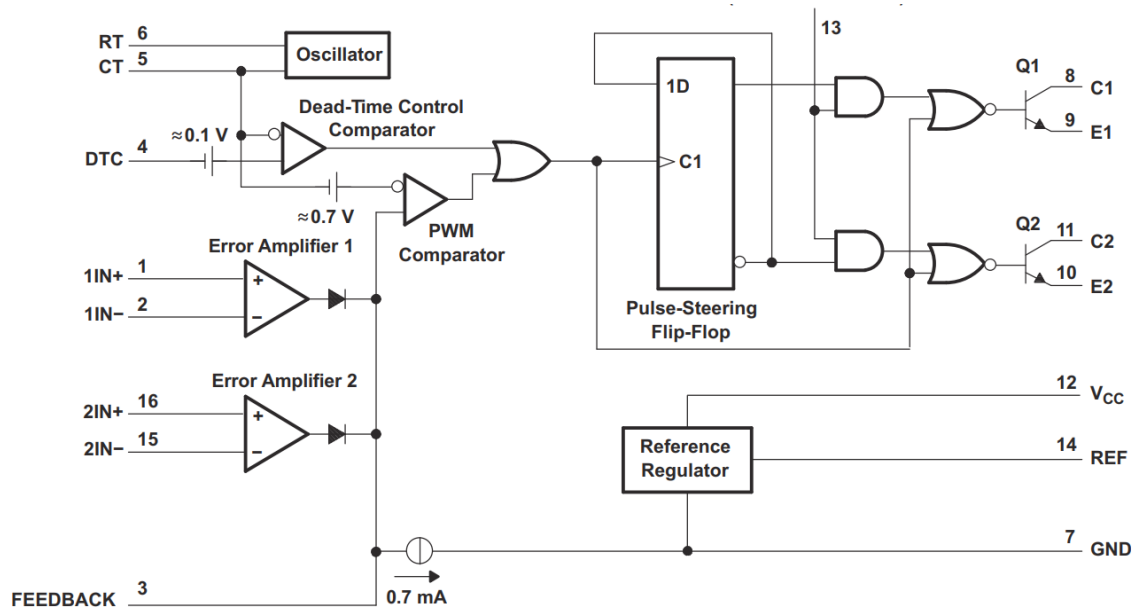


Figure 29. TL494 block diagram (Reprinted from [27,10])

TL494 consists of a sawtooth oscillator, a PWM comparator, two error amplifiers, a 5V voltage regulator, etc. The supply voltage for TL494 ranges from 7V to 40V, the voltage regulator can supply 10mA current for additional circuits, each open collector output can sink a maximum of 200mA current, and the recommended oscillator frequency is 1kHz–300kHz [27,4;27,10]. Grounding pin 4 of the dead time comparator ensures the duty cycle control from ~3% to 100% [27,11]. When the pulse-steering flip flop is disabled, the output logic of the PWM comparator appears at both Q1 and Q2 input at the same time, meaning both Q1 and Q2 outputs have same characterized PWM signals. The pulse-steering flip flop can be disabled by connecting the output control pin 13 to the ground [27,12].

This PWM based voltage measurement circuit block diagram is illustrated in figure 30.

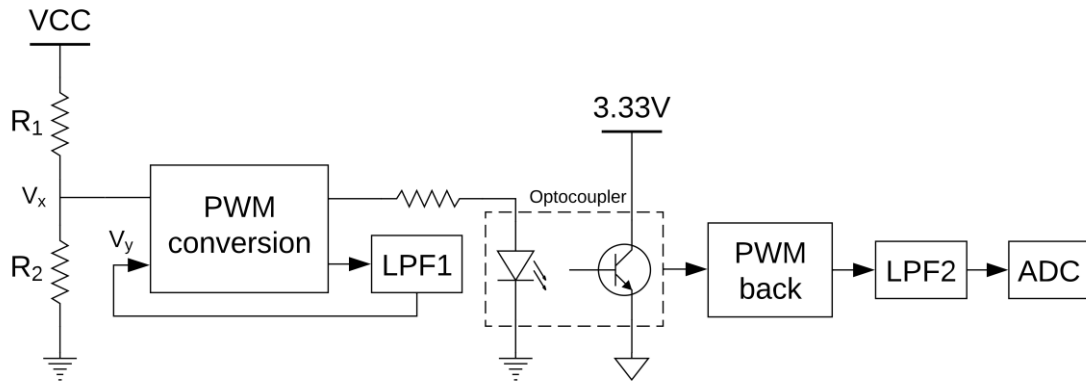


Figure 30. The block diagram of the PWM based voltage measurement

A voltage divider is formed from the input voltage V_{CC} . V_x voltage is fed to TL494, and TL494 converts this voltage into the corresponding PWM signal. Both Q1 and Q2 output the same PWM signals. Q1 drives the optocoupler, and Q2 PWM signal is fed to low pass filter 1 (LPF1) to convert the PWM signal back to the analog voltage V_y . V_x and V_y voltages are fed to an error amplifier. The output of the error amplifier controls the PWM comparator. Error amplifier outputs higher voltage when the difference between V_x and V_y is higher. The duty cycle of the PWM increases with higher V_x values. A higher duty cycle means a higher DC component of the PWM signal. For example, V_x is 1V, and the error amplifier would manipulate the duty cycle to make the V_y very close to the V_x value. The duty cycle is higher at first, and as V_y moves to the value of V_x , the duty cycle keeps going lower. Then, at a certain duty cycle, V_y is very close to V_x , and the duty cycle stabilizes at this point. For $V_x = 1V$, the corresponding stabilized PWM duty cycle may be 30%. If the V_x becomes 2V, the same scenario occurs, and the corresponding stabilized PWM duty cycle could be 70%, for example.

As said above, Q1 follows the same PWM signal of Q2 output all the time. The identical pulses appear at the emitter of the optocoupler. These pulses are converted back to the PWM. The duty cycles of the PWM signals in both the main and measurement sides should be equal. The measurement side PWM is converted back to analog using low pass filter 2 (LPF2). The ADC of the

microcontroller measures this voltage which allows the microcontroller to calculate the input voltage. The conversion to the analog voltage on the measurement side can be avoided if the input capture is available in the microcontroller. The microcontroller can measure the duty cycle using the input capture that can be used to calculate the input voltage [28].

The characteristics of the sawtooth oscillator and the PWM comparator of the TL494 IC were measured using an oscilloscope. The low and high levels of the sawtooth wave are approximately 156mV and 2.8V respectively. The duty cycle of the PWM signal increases approximately linearly from 4.44% to 100% with 0.92V to 3.51V at the feedback pin 3. There is no effect on the duty cycle below 0.92V at feedback pin 3.

The voltage measurement circuit is shown in figure 31 with key components inside the TL494 block. Alongside TL494, U4A, U4B, U6 op-amps, U5 comparator, and U9 optocoupler were used. LM324N op-amps and LM393 comparator were selected as they were available in the laboratory, met the voltage range, and were among the cheapest options. This circuit was built on the breadboard to measure 16V–30V.

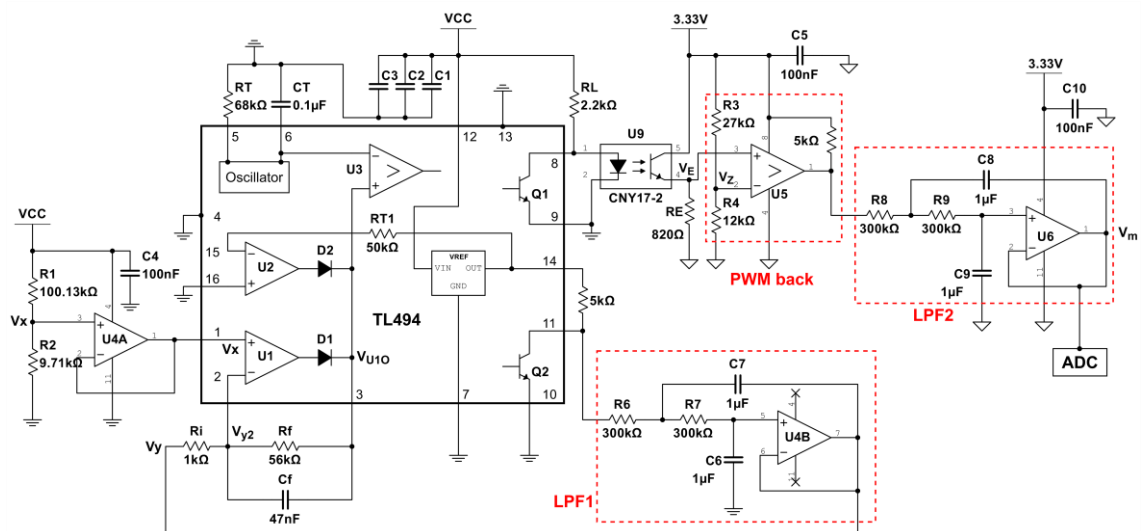


Figure 31. PWM based voltage measurement circuit

The presence of diodes in front of U1 and U2 error amplifiers can be seen connecting together at pin 3. U1 error amplifier was configured as a non-inverting amplifier to check if it had a diode voltage drop at pin 3. It was confirmed that U1 error amplifier works as per the non-inverting configuration without a diode voltage drop at pin 3. U2 was configured as per the datasheet [27,8] so that it does not drive pin 3. Pulse-steering flip flop was disabled by grounding pin 13. Pin 4 was grounded as no additional dead time was utilized. The oscillator frequency was set up using RT and CT. RT and CT values were derived from the datasheet's Oscillator Frequency and Frequency Variation vs Timing Resistance graph [27,7]. RT = 68kΩ and CT = 0.1μF make the oscillator frequency to be 198 Hz. C₁ = 10nF, C₂ = 100nF, C₃ = 47μF were used as bypass capacitors.

As it was observed that pin 3 needs 0.92V–3.51V at pin 3 for controlling the duty cycle, the input voltage was scaled down to this range by a voltage divider formed by R₁ and R₂. At 16V, $V_x = \frac{16V \times R_2}{R_2 + R_1} = \frac{16V \times 9.71k\Omega}{9.71k\Omega + 100.13k\Omega} = 1.414V$ and at 30V, $V_x = \frac{30V \times 9.71k\Omega}{9.71k\Omega + 100.13k\Omega} = 2.652V$. U4A op-amp buffer measures V_x voltage.

A second order Sallen-Key LPF1 was built using the U4B op-amp utilizing the online calculator from OKAWA Electric Design [17]. The input to LPF1 is taken from the Q2 output with a 5kΩ pullup resistor that is connected to the internal 5V voltage regulator of TL494. R₆ values lower than 300kΩ were loading the Q2 PWM signal. For example, PWM high value was reduced by 100mV when R₆ was 100kΩ. The reduction was much more at lower R₆ values. The PWM high value was almost stable at R₆ = 300kΩ. R₆ = R₇ = 300kΩ and C₆ = C₇ were used during the measurements. Performance was observed at different capacitor values. The pole frequency can be calculated using equation (7) when C₆ = C₇ = 1μF are used.

$$f_c = \frac{1}{2\pi\sqrt{R_6 R_7 C_6 C_7}} = \frac{1}{2\pi\sqrt{300k\Omega \times 300k\Omega \times 1\mu F \times 1\mu F}} = 0.53Hz$$

The converted analog voltage out of LPF1 is taken to the error amplifier formed by the U1 op-amp. This error amplifier ensures $V_x \approx V_{y2}$; however, as V_y is

LPF1 output, the U1 error amplifier keeps manipulating the duty cycle that makes the V_y value close to V_{y2} . It could be approximated that V_y is equal to V_x . R_i and R_f values were chosen such that U1 outputs higher than 3.51V to make the duty cycle 100% at a high difference between V_x and V_y . For example, at $V_x = 2V$ and $V_y = 1.5V$, U1 output would be according to equation (8):

$$V_{U1O} = V_x - \frac{(V_y - V_x)R_f}{R_i} = 2V - \frac{(1.5V - 2V)56k\Omega}{1k\Omega} = 30V$$

Similarly, at $V_x = 2V$ and $V_y = 1.99V$, U1 output would be:

$$V_{U1O} = 2V - \frac{(1.99V - 2V)56k\Omega}{1k\Omega} = 2.56V$$

The output voltages of U1 are within 0.92 and 3.51V when V_y is very close to but less than V_x . U1 saturates to 0V when V_y exceeds V_x . This is how U1 regulates the PWM signal, and so does the LPF1 output.

On the upper side, Q1 drives the U9 CNY17-2 optocoupler LED with an R_L resistor connected to VCC. Optocoupler LED voltage varies between 1.16V and 1.32V for 6mA to 13mA current at 25°C [29,5]. $R_L = 2.2k\Omega$ LED resistor was used. It makes the LED current to be approximately $\frac{16V-1.25V}{2.2k\Omega} = 6.7 mA$ at 16V VCC and $\frac{30V-1.25V}{2.2k\Omega} = 13 mA$ at 30V at 25°C.

Optocoupler's CTR varies between 63% and 125% [29,1], and the normalized CTR is about 0.76 according to the normalized CTR graph in the datasheet [29,6] at 75°C. The minimum CTR at 75°C can be calculated as per equation (2) assuming 10% aging and 20% negative tolerance factors:

$$CTR_{min} = 63 \times 0.76 \times 0.9 \times 0.8 = 34.47\%$$

This makes the minimum emitter current = $34.47\% \times 6.7mA = 2.31mA$, and the minimum voltage across the $R_E = 820\Omega$ is $2.31mA \times 820 = 1.89V$. However, the voltage across R_E was close to 3.2V during the breadboard measurement.

The measurement side circuit was powered by 3.33V. U5 comparator is used to construct the PWM signal on the measurement side so that high and low levels of the PWM signal are stable, have sharp rise and fall characteristics. R_3 and R_4 voltage divider makes $V_z = \frac{3.33V \times R_4}{R_4 + R_3} = \frac{3.33V \times 12k\Omega}{12k\Omega + 27k\Omega} = 1.025V$. V_z voltage is connected to the inverting input and the emitter output V_E is connected to the non-inverting input of the comparator meaning the comparator outputs high when there is a signal at the optocoupler. In other words, the constructed PWM signal on the measurement side is in phase with TL494 generated PWM signals. The output of the comparator was connected to 3.33V with a $5k\Omega$ pullup resistor, and the comparator outputs a 3.33V PWM signal.

The PWM signal on the measurement side is connected to the input of LPF2 to convert it back to the analog voltage that is measured by the ADC of a microcontroller. LPF2 has the same characteristics as LPF1.

Assume the duty cycle of the Q2 PWM is D_{on1} and the duty cycle of the U5 comparator output PWM is D_{on2} . D_{on1} and D_{on2} are not in percentage; they range from 0 to 1. Ideally $D_{on1} = D_{on2}$. The DC component of the PWM signal in the measurement side using equation (3) is,

$$V_m = (V_{OH2} - V_{OL2})D_{on2} + V_{OL2}$$

$$D_{on2} = \frac{V_m - V_{OL2}}{V_{OH2} - V_{OL2}}$$

Similarly, the DC component of Q2 PWM is,

$$V_y = (V_{OH1} - V_{OL1})D_{on1} + V_{OL1}$$

$$V_y = (V_{OH1} - V_{OL1}) \frac{V_m - V_{OL2}}{V_{OH2} - V_{OL2}} + V_{OL1} \quad (18)$$

If the duty cycle is used for the measurement, then V_y can be found by replacing D_{on1} with D_{on2} .

$$V_y = (V_{OH1} - V_{OL1})D_{on2} + V_{OL1} \quad (19)$$

Here, V_m = Measured voltage on the isolation side

V_{OH2} = High voltage level of U5 comparator PWM

V_{OL2} = Low voltage level of U5 comparator PWM

D_{on2} = Duty cycle of U5 comparator PWM ranging from 0 to 1

V_{OH1} = High voltage level of Q2 PWM

V_{OL1} = Low voltage level of Q2 PWM

D_{on1} = Duty cycle of Q2 PWM ranging from 0 to 1

V_y is approximately equal to V_x . Therefore, the input voltage can be calculated as follows:

$$V_x = V_y = \frac{VCC \times R_2}{R_1 + R_2}; \Rightarrow V_y(R_1 + R_2) = VCC \times R_2$$

$$VCC = \frac{V_y(R_1 + R_2)}{R_2} \quad (20)$$

The measured parameters are, $V_{OH1} = 4.92V$; $V_{OL1} = 0.63V$; $V_{OH2} = 3.28V$; $V_{OL2} = 0.01V$.

A calculation can be presented. Assume the ADC reads $V_m = 1V$, then by equation (18):

$V_y = (4.92V - 0.63V) \frac{1V - 0.01V}{3.28V - 0.01V} + 0.63V = 1.93V$. The corresponding input voltage, $VCC = \frac{1.93V(9.71k\Omega + 100.13k\Omega)}{9.71k\Omega} = 21.83V$. R_1 and R_2 are required to be in tight tolerance because this impacts the measurement result greatly.

In summary, the input voltage information is converted to a PWM signal by TL494. This PWM signal is passed to the measurement side through the optocoupler. The PWM signal is converted back to analog voltage using LPF2, and this voltage is measured by an ADC. The feedback from LPF1 eliminates

the equation dependency on sawtooth wave frequency, which offers less measurement error in frequency variation, and feedback should also help attain less measurement error in temperature variation.

3.2 LED Circuits

This section excludes the model numbers of the LEDs and constant current IC due to the confidentiality of the company. The LED card consists of 3000K and 5000K color temperature LEDs. Each type consists of 36 LEDs. Each LED channel is divided into six parallel branches, each branch containing six LEDs in series. The nominal LED branch current is 65mA at 21V supply voltage and full brightness. The peak LED branch current is higher at higher supply voltage, but the circuit maintains an average current of 65mA by 3kHz PWM signal through each LED branch at full brightness. The duty cycle of the PWM signal is lowered to achieve lower brightness. The 5000K LED channel enters emergency mode when the PWM signal for the 5000K LED channel is unavailable from the microcontroller. Both 3000K and 5000K LEDs that are used in this LED card have identical current voltage relationships and maximum allowable current. The LED specifications are derived from the datasheet in the calculation.

3.2.1 3000K LED Channel

The circuit is shown in figure 32. This circuit does not include the last four branches because they have the same components and characteristics as the first two branches.

The PWM signal from the microcontroller is passed through the TCMT1103 optocoupler to the LED circuit. The LED circuit is in switch mode, as shown in subsection 2.6.4. The N-channel MOSFET was chosen based on its capability of handling max LED branch current, threshold voltage $\leq 3.5V$, so that high load resistor for R_{E1} can be avoided, and low $R_{DS(ON)}$. The threshold voltage V_{TH} of

the MOSFET varies from 1V–3V, and the maximum gate-source voltage is ± 20 V.

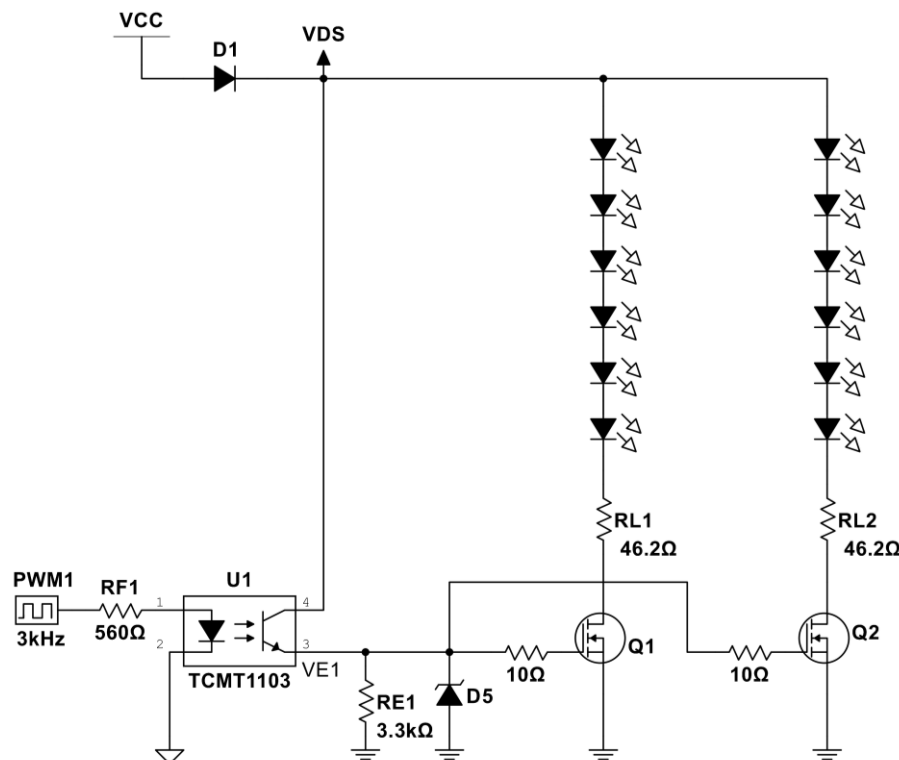


Figure 32. 3000K LED channel circuit

The high level of the PWM signal drives the optocoupler LED that causes current in the emitter of the optocoupler. The gate voltages of the MOSFETs are taken from the optocoupler's emitter voltage V_{E1} . The current flows through the LED branches when the PWM high level is available. When the PWM low level appears, it does not activate the optocoupler's emitter, so the emitter is at 0V which turns off the MOSFETs causing no current flow through the LED branches. MOSFET gates are discharged via 10Ω gate and R_{E1} resistors during the low period of the PWM signal. Each LED branch has its own MOSFET switch. As all MOSFET gates are connected to the optocoupler's emitter voltage through gate resistors, the PWM signal controls all LED branches simultaneously. All LED branches ideally have the same characteristics, as each branch has the same components.

The 3.3V microcontroller generates a minimum 2.9V high level for the PWM signals. Optocoupler's forward LED voltage at 3.2mA is approximately 1.12V at 25 °C [6,4]. To drive 3.2mA current through the optocoupler LED, it requires $\frac{2.9V-1.12V}{3.2mA} = 556.25\Omega$ resistor. A close value $R_{F1} = 560\Omega$ was used in this case. The CTR calculation for 3.2mA current for the optocoupler's LED has been presented in section 2.1. A $R_{E1} = 3.3k\Omega$ resistor is between the optocoupler's emitter and the ground. The minimum optocoupler's emitter current $I_{E1min} = \frac{CTR_{min}}{100} \times 3.2mA = 0.372 \times 3.2mA = 1.19mA$ at 75°C. Therefore, the optocoupler's minimum emitter voltage is $I_{E1min} \times R_{E1} = 1.19mA \times 3300\Omega = 3.93V$ that stays above the MOSFET's threshold voltage during the operation. The optocoupler's minimum emitter voltage at 25°C, excluding the aging and tolerance factors, is $0.825 \times 3.2mA \times 3300\Omega = 8.71V$. A 15V D5 Zener diode is used to clamp the gate voltages of the MOSFETs if the CTR causes the emitter voltage of the optocoupler to exceed 15V.

LED branches are powered from the VDS net. LED branch resistance is calculated based on full brightness at 21V supply voltage and 65mA current. The 3000K LED forward voltage is typically 2.88V at 65mA current according to the datasheet. $R_{DS(on)}$ of the MOSFET is below 0.1Ω at 1A drain current and 4.5V gate to source voltage. The resistor R_{L1} can be calculated approximately using equation (12),

$$R_{L1} = \frac{VCC - nV_f - 0.71V}{I_{max}} - R_{DS(on)} = \frac{21V - 6 \times 2.88V - 0.71V}{65mA} - 0.1 = 46.2\Omega$$

The relationship between the LED current and brightness for both 3000K and 5000K LED types is linear at different segments, according to the datasheets. The overall relationship is considered to be linear in the calculation.

The brightness can be controlled linearly by changing the PWM duty cycle linearly. For example, a 10% duty cycle keeps the LEDs on for 10% time in a period, causing an average current of $0.1 \times 65mA = 6.5mA$ at 21V supply voltage. The 6.5mA LED current denotes 10% brightness; similarly, 32.5mA LED current represents 50% brightness.

As the LED forward voltage does not change linearly with LED current, LED forward voltages were measured on an LED card PCB at different current levels.

Assume the LED forward voltage is 3.2V at 30V supply voltage. Then, the LED branch current by equation (11) is:

$$I_{max} = \frac{30V - 6 \times 3.2V - 0.71V}{46.2\Omega + 0.1\Omega} = 218mA$$

It is more than the nominal current at full brightness. It can be transformed into 65mA current by feeding $\frac{65mA \times 100}{218mA} = 29.8\%$ PWM duty cycle. From this 29.8% duty cycle point, the brightness can be controlled linearly at 30V. For example, the required PWM duty cycle is $0.1 \times 29.8\% = 2.98\%$ to achieve 10% brightness at 30V. The same method is used for supply voltage above 21V up to 30V for brightness control. At voltages lower than 21V, the LED branch current would follow the equation (11) approximately meaning the brightness would reduce with supply voltage reduction.

The power ratings of the series resistors in the LED branches were 0.25W and 0.33W. As shown above, the LED branch current may go as high as 218mA at 30V, the power dissipation of R_{L1} is $(0.218^2)mA \times 46.2\Omega = 2.2W$ at PWM on time, which exceeds the power rating. Therefore, R_{L1} was divided into nine 0.33W 4.7 Ω series resistors in series with three 0.25W 4700 Ω , 27 Ω , 4.7 Ω parallel resistors. Power dissipation through each 0.33W 4.7 Ω resistor is $0.218^2 \times 4.7 = 0.223W$ at PWM on time at 30V supply voltage.

In parallel resistors, 4700 Ω and 27 Ω form an equal resistance of $\frac{4700\Omega \times 27\Omega}{4700\Omega + 27\Omega} = 26.85\Omega$. The current through 0.25W 4.7 Ω resistor is $\frac{218mA \times 26.85\Omega}{4.7\Omega + 26.85\Omega} = 0.185mA$, and the power dissipation is $(0.185^2)mA \times 4.7\Omega = 0.161W$ that is within the 0.25W power rating. The other 4700 Ω and 27 Ω resistors dissipate less than 0.161W power.

3.2.2 5000K LED Channel

The design for the 5000K LED channel is the same as the 3000K LED channel in switch mode operation as both LED types have identical I-V curves and maximum allowable current. The addition to the 5000K LED channel is its operation in the case of the missing PWM signal. The circuit is shown in figure 33, and the last four LED branches are not shown again as they have the same component values as the first two branches.

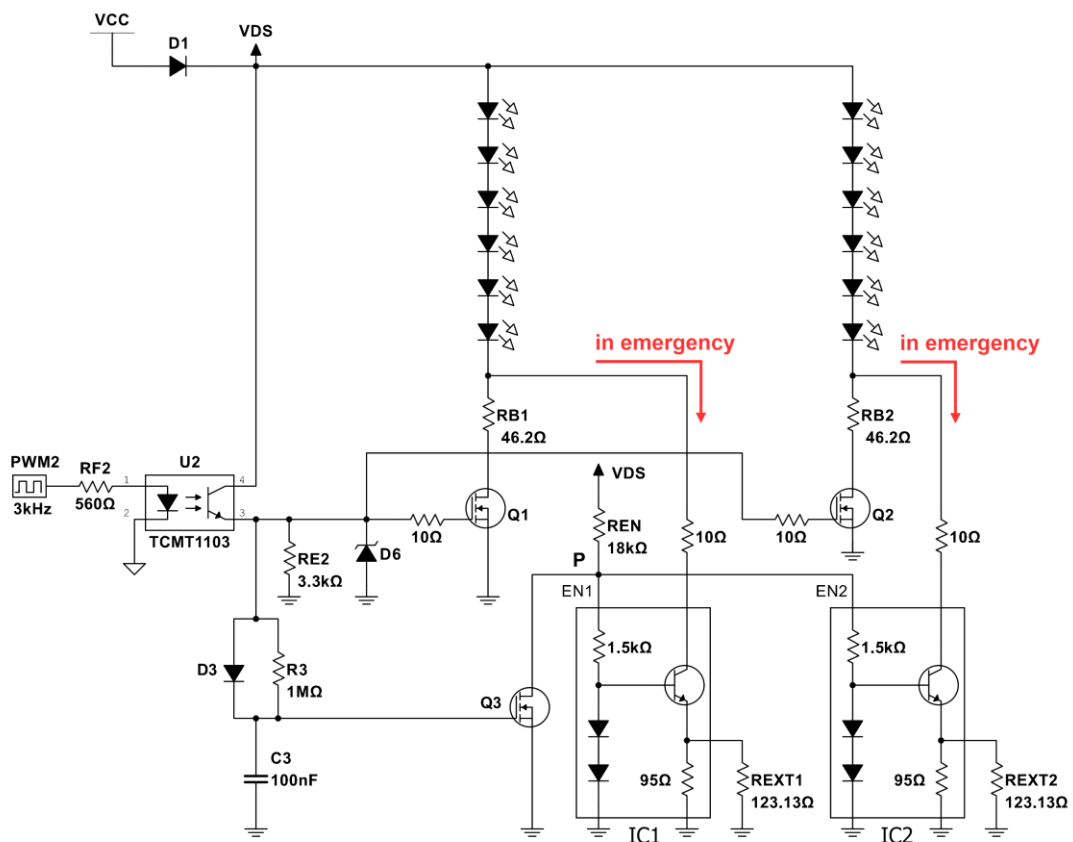


Figure 33. 5000K LED channel circuit

The 5000K LED channel switches LED branches with 13mA in CC mode, which is 20% brightness, when the PWM signal is not available for the 5000K LED channel. The constant current IC based on the single transistor was used here. This IC has a nominally 95Ω resistor between the emitter and ground and a nominally 1.5kΩ resistor between the EN pin and the base of the transistor. The

minimum current gain β is 200. EN pins of these ICs are connected together at point P which connects the drain of Q3 N-channel MOSFET. The same MOSFET as the LED branch MOSFETs was used for Q3. There is an R_{EN} resistor between the VDS net and point P. The collectors of the CC ICs connect to the cathode of the last LEDs of the branches via 10Ω resistors. The activation and deactivation of the Q3 MOSFET using the D3 and R_3 combination was configured as per the suggestion from the company. During the startup, Q3 MOSFET is inactive. PWM signal charges the C_3 capacitor mostly through the D3 diode and turns on the Q3 MOSFET when the C_3 voltage exceeds the Q3 MOSFET threshold voltage. When Q3 MOSFET is active, it pulls the P point close to 0V making the CC ICs inactive, so the LED branches work in switch mode. In the event of the missing PWM signal, C_3 capacitor slowly discharges through the R_3 resistor, and Q3 becomes inactive once C_3 voltage falls below the threshold voltage. It activates the CC ICs, and 13 mA current flows through each LED branch, and LED branch MOSFETs are inactive during this time.

From equation in subsection 2.6.1, the base needs to have $I_B \geq \frac{13\text{mA}}{200} = 65\mu\text{A}$ to achieve 13mA current. As the base currents are shared from point P equally to each CC IC, the total base current needs to be $\geq 6 \times 65\mu\text{A} = 390\mu\text{A}$. The datasheet of the CC IC does not include the diode voltage drop. Assume the total diode voltage drop is 1.6V, and the total current through R_{EN} is $540\mu\text{A}$, so each $1.5\text{k}\Omega$ base resistor draws $\frac{540\mu\text{A}}{6} = 90\mu\text{A}$. The voltage at point P is $1.6\text{V} + (90\mu\text{A} \times 1.5\text{k}\Omega) = 1.735\text{V}$. It makes $R_{EN} = \frac{16.8\text{V} - 0.71\text{V} - 1.735\text{V}}{540\mu\text{A}} = 26583\Omega$ at 16.8V supply voltage.

It required $R_{EN} = 18\text{k}\Omega$ and $R_{EXT1} = 123.13\Omega$ to achieve 13mA currents through the branches in emergency mode.

4 Results

This chapter includes all measurement results. The measurement results are presented in two separate sections that differentiate the isolated DC voltage measurement results and LED branch results. This includes breadboard measurement results for isolation amplifier, linear optocoupler, and PWM based voltage measurement circuits, and TL431 based voltage measurement circuit, LED circuits on PCBs of the LED card. Arduino MKR WiFi 1010, digital multimeter, and KEYSIGHT InfiniiVision DSOX2014A oscilloscope were used in the measurement.

4.1 Isolated DC Voltage Measurement Circuits

All components for linear optocoupler, isolation amplifier, and PWM based voltage measurement circuits were through hole except AMC1311B and TLV9351 ICs. AMC1311B and TLV9351 were soldered on their footprints, and wires were soldered on traces coming out of the pins to set them up for breadboard circuits. Arduino was used to take voltage measurements wherever it was deemed necessary to make the results comparable to other microcontrollers taken measurements. The range between the hundredths and thousandths place was fluctuating during the measurements with Arduino. The most frequent number or the average of frequent numbers was taken as the measured value. However, the values were mostly stable on the digital multimeter.

4.1.1 Linear Optocoupler Based Voltage Measurement

Table 1 lists the measurement results below. The measured voltage is converted back to supply voltage using equation (14). The measurements were taken with the digital multimeter. After the first measurement, the measurements were retaken by replacing the IL300 linear optocoupler with another optocoupler of the same model to observe IL300 IC to IC variation. All other components were same.

Table 1. Linear optocoupler based voltage measurement results

1st IL300 IC					2nd IL300 IC				
Power supply voltage (V)	Isolated measured voltage (V)	Converted power supply voltage (V)	Error voltage (mV)	Error (%)	Power supply voltage (V)	Isolated measured voltage (V)	Converted power supply voltage (V)	Error voltage (mV)	Error (%)
16	1.014	16.76	764.53	4.78	16	1.073	17.74	1739.98	10.87
17	1.077	17.81	806.11	4.74	17	1.14	18.85	1847.70	10.87
24	1.521	25.15	1146.79	4.78	24	1.61	26.62	2618.24	10.91
25	1.585	26.20	1204.91	4.82	25	1.678	27.74	2742.48	10.97
26	1.648	27.25	1246.49	4.79	26	1.745	28.85	2850.20	10.96
29	1.839	30.40	1404.31	4.84	29	1.945	32.16	3156.81	10.89
30	1.903	31.46	1462.42	4.87	30	2.014	33.30	3297.60	10.99

Measurements were taken from 16V to 30V with 1V step. Measurement results show that there are differences between two photodiode currents yielding 0.76V to 1.46V difference with the power supply voltage in the case of IL300 IC1. For instance, at 30V power supply, the input photodiode current is $\frac{30V}{330k\Omega} = 90.9\mu A$ and the output photodiode current is $\frac{1.903V}{19.96k\Omega} = 95.34\mu A$. The voltage error increased with an increase in power supply voltage.

Same characteristics are observed for IL300 IC2 also. However, the error voltage differs significantly from IL300 IC1. Here the error percentage is about 6% higher than the first IC.

4.1.2 Isolation Amplifier Based Voltage Measurement

The measurements were taken by the Arduino. The measurements were taken in two parts as linear optocoupler with two different AMC1311B ICs. Other components were left unchanged. Table 2 shows the measurement results. The measurement results are converted back to the power supply voltage using equation (15).

Table 2. Isolation amplifier based voltage measurement results

1 st AMC1311B IC					2 nd AMC1311B IC				
Power supply voltage (V)	Isolated measured voltage (V)	Converted power supply voltage (V)	Error voltage (mV)	Error (%)	Power supply voltage (V)	Isolated measured voltage (V)	Converted power supply voltage (V)	Error voltage (mV)	Error (%)
16	1.019	16.05	48.50	0.30	16	1.022	16.10	95.75	0.60
17	1.086	17.10	103.70	0.61	17	1.086	17.10	103.70	0.61
24	1.522	23.97	-29.62	0.12	24	1.522	23.97	-29.62	0.12
24.8	1.58	24.88	83.83	0.34	24.8	1.582	24.92	115.33	0.47
24.85	1.585	24.96	112.58	0.45	24.85	1.581	24.90	49.58	0.20
24.9	1.589	25.03	125.58	0.50	24.9	1.58	24.88	-16.17	0.06
24.95	1.587	24.99	44.08	0.18	24.95	1.59	25.04	91.33	0.37
25	1.582	24.92	-84.67	0.34	25	1.594	25.10	104.32	0.42
26	1.65	25.99	-13.72	0.05	26	1.65	25.99	-13.72	0.05
27	1.712	26.96	-37.26	0.14	27	1.715	27.01	9.99	0.04
28	1.782	28.07	65.19	0.23	28	1.78	28.03	33.69	0.12
29	1.847	29.09	88.89	0.31	29	1.845	29.06	57.39	0.20
30	1.905	30.00	2.35	0.01	30	1.91	30.08	81.09	0.27

The results show that most converted power supply voltages are within 100mV of actual voltage levels. Both AMC1311B ICs show similar characteristics. Both measurements show the error is within 0.61%.

4.1.3 TL431 Based Voltage Measurement

The voltage at point Z was measured to be 5.023V. The value remained almost the same from 16V to 30V power supply. The measurements were taken with only emergency mode on with 10mA current through the 5000K LED branches. The microcontroller of the subcircuit was used for the measurements. D1 diode voltage was about 0.705V, and the reference voltage V_{ref} was measured to be 2.43V. CTR values changed with change in power supply voltage and varied with another LED card. CTR values were more stable with I_{KA} current more than 8mA. CTR values were calculated on two different LED cards. The average CTR value at 21V, 24V, 29V, and 30V from these two LED cards was calculated to be 145.8%. The converted voltage results using this average CTR value are shown in table 3 and 4 for two LED cards. The measured voltages were converted to the power supply voltage using equations (1), (16) and (17).

Table 3. TL431 based circuit measurement results on the first LED card

First LED card								
Power supply voltage (V)	I_{KA} (mA)	Measured voltage (V)	Optocoupler emitter current (mA)	CTR (%)	Converted I_{KA} with average 145.8% CTR (mA)	Converted power supply voltage (V)	Error voltage (mV)	Error (%)
16	4.614	0.527	6.433	139	4.411	15.55	-446.78	2.79
17	5.068	0.584	7.121	140	4.883	16.59	-409.01	2.41
21	6.887	0.819	9.988	145	6.849	20.92	-82.71	0.39
24	8.250	1.001	12.213	148	8.374	24.27	273.20	1.14
24.8	8.614	1.040	12.687	147	8.699	24.99	187.51	0.76
24.85	8.637	1.042	12.713	147	8.718	25.03	177.94	0.72
24.9	8.659	1.046	12.758	147	8.748	25.10	195.33	0.78
24.95	8.682	1.048	12.785	147	8.767	25.14	185.76	0.74
25	8.705	1.059	12.910	148	8.852	25.32	324.45	1.30
29	10.523	1.294	15.778	150	10.819	29.65	650.75	2.24
30	10.978	1.348	16.439	150	11.272	30.65	648.09	2.16

Table 4. TL431 based circuit measurement results on the second LED card

Second LED card								
Power supply voltage (V)	I_{KA} (mA)	Measured voltage (V)	Optocoupler emitter current (mA)	CTR (%)	Converted I_{KA} with average 145.8% CTR (mA)	Converted power supply voltage (V)	Error voltage (mV)	Error (%)
16	4.614	0.495	6.031	131	4.135	14.95	-1053.27	6.58
17	5.068	0.550	6.710	132	4.601	15.97	-1028.98	6.05
21	6.887	0.787	9.595	139	6.579	20.32	-675.73	3.22
24	8.250	0.967	11.793	143	8.087	23.64	-360.25	1.50
24.8	8.614	1.013	12.356	143	8.472	24.49	-311.16	1.25
24.85	8.637	1.015	12.383	143	8.491	24.53	-320.73	1.29
24.9	8.659	1.018	12.410	143	8.509	24.57	-330.29	1.33
24.95	8.682	1.021	12.445	143	8.534	24.62	-326.38	1.31
25	8.705	1.024	12.490	143	8.564	24.69	-309.00	1.24
29	10.523	1.256	15.322	146	10.506	28.96	-36.61	0.13
30	10.978	1.309	15.965	145	10.947	29.93	-66.23	0.22

The results below 21V can be ignored as the LEDs are operated with maximum 100% PWM duty cycle. The first LED card shows that power supply voltage conversion is higher than the actual voltage except at 21V. It has a maximum of 650.75mV difference with the actual voltage making 2.24% error.

The results are the opposite for the second LED card. The conversion results in maximum 675.3mV lower than the actual voltage making maximum 3.22% error.

4.1.4 PWM Based Voltage Measurement

A thorough measurement was taken for this circuit. A high speed optocoupler VOH1016AD was used to compare the result with the standard optocoupler CNY17-2. High speed optocoupler was more accurate than the standard optocoupler at every conducted operating frequency because it has better rise and fall characteristics than the standard optocouplers. The circuit was operated with 1.27kHz, 408Hz, and 198Hz frequencies. The circuit with the standard optocoupler performed better at 198Hz and 408Hz than at 1.27kHz. Measurements taken with 198Hz operating frequency are presented in this subsection. Other measurement results are shown in appendix 1.

Referring to the circuit shown in figure 31, waveforms of TL494 sawtooth wave, Q2 PWM output, optocoupler's emitter, U5 comparator output, LPF1 output, and LPF2 output were captured using the oscilloscope. Figure 34 shows the sawtooth wave, Q2 PWM output, and U5 comparator output at 24V supply voltage. Yellow, green, and blue waveforms represent the sawtooth wave, Q2 PWM output, and U5 comparator output respectively. U5 comparator duty cycle is bit higher than the Q2 PWM output because it stays high approximately $8\mu\text{s}$ longer than the Q2 PWM due to the optocoupler's slow fall response.



Figure 34. Sawtooth wave, Q2 PWM output, and U5 comparator output waveforms

Figures 35 and 36 show the rise and fall characteristics of Q2 PWM, optocoupler's emitter, and U5 comparator PWM output respectively at 24V supply voltage. Yellow, green, and blue waveforms represent Q2 PWM, optocoupler's emitter output, and U5 comparator output respectively.

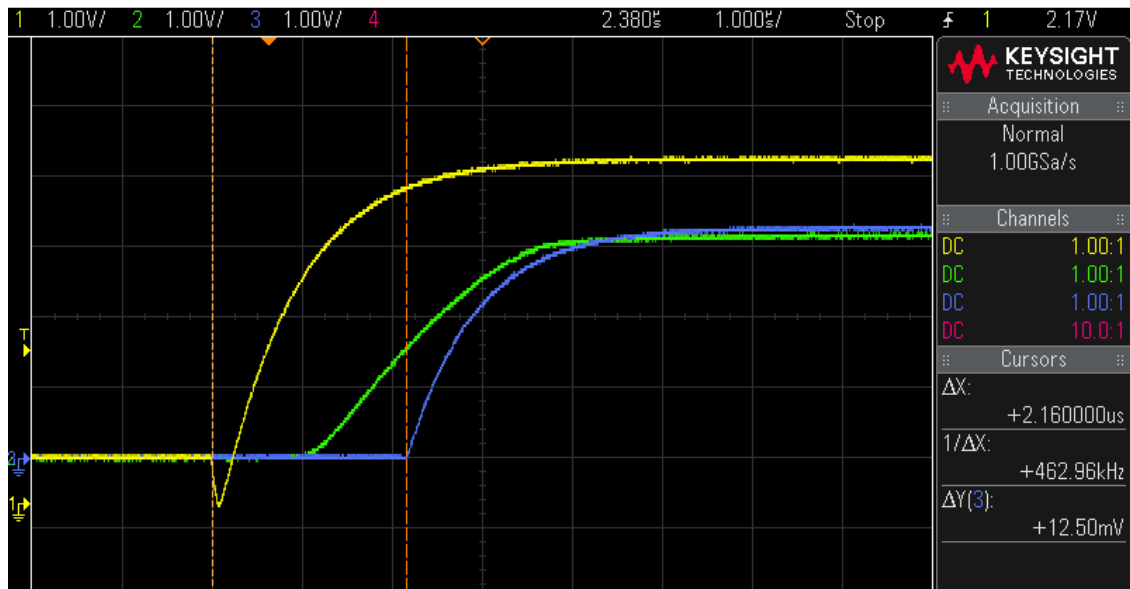


Figure 35. Q2 PWM, optocoupler's emitter, and U5 comparator rise characteristic

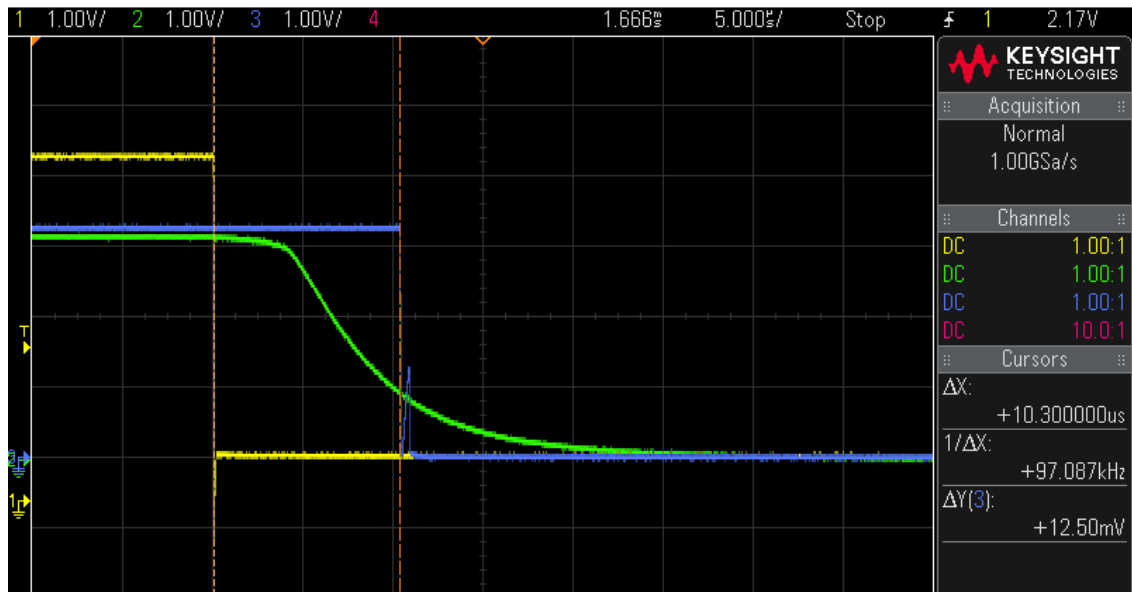


Figure 36. Q2 PWM, optocoupler's emitter, and U5 comparator fall characteristic

Figures 35 and 36 show that both Q2 PWM and U5 comparator PWM have similar fall and rise behaviour. Optocoupler's phototransistor has shorter turn-on time than turn-off time.

The output of LPF2 had ringing and oscillation at PWM fall and rise. LPF1 output also had ringing but the waveform looks better than LPF2 output. Figure 37 shows the scenario, and figure 38 shows a closer view. Yellow, green, and blue waveforms represent Q2 PWM, LPF1 output, and LPF2 output respectively.

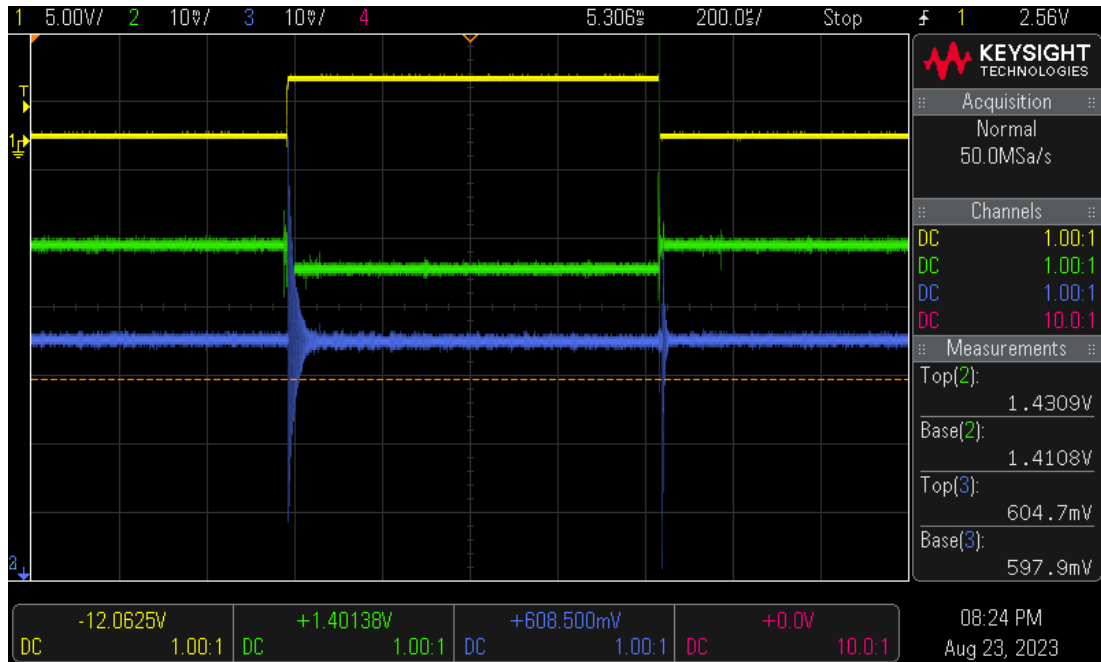


Figure 37. Ringing and oscillation on LPF1 and LPF2 waveforms

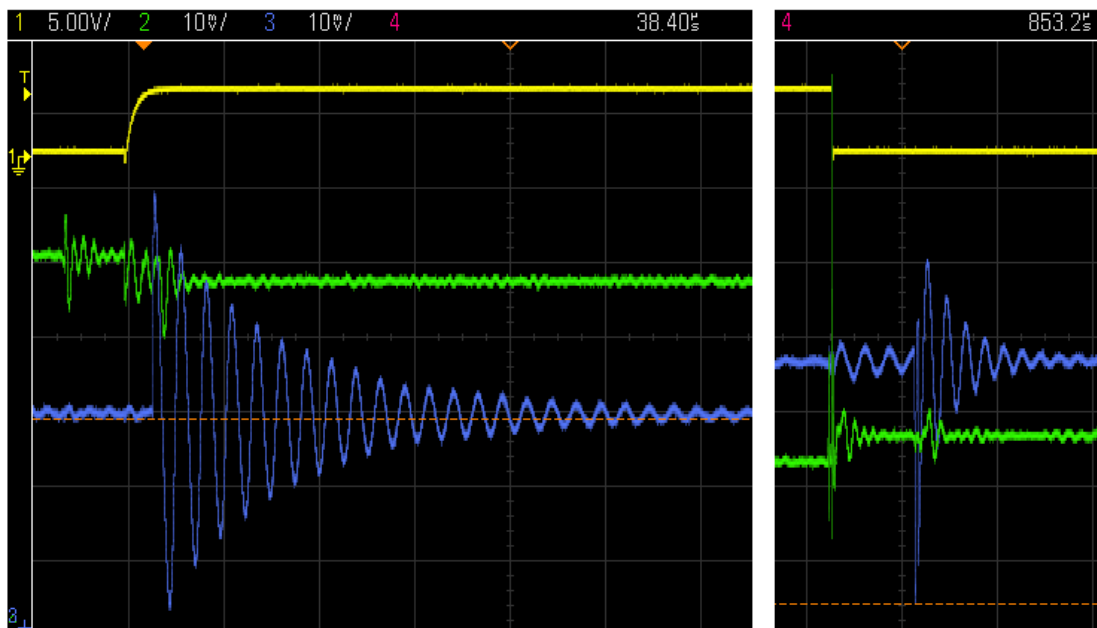


Figure 38. Closer view of ringing and oscillations

Figure 38 shows that LPF2 takes about $70\mu\text{s}$ to settle during the rise of Q2 PWM but takes about $10\mu\text{s}$ to settle during the fall of Q2 PWM.

Measurements were taken with two sets of ICs to observe how IC to IC variation affects the accuracy. The high and low voltage levels were 4.92V and 0.63V respectively for Q2 PWM output. The PWM output of the U5 comparator had 3.28V high voltage and 0.01V low voltage. The measurements were taken with 1V step from 16V to 30V and some measurements with 50mV steps. The voltage was measured using the Arduino, and the oscilloscope was used to measure the duty cycle of the U5 comparator PWM. The values are shortened to two decimals mostly. Measurement results of the first ICs set are presented in table 5 using equations (18), (19), (20).

Table 5. PWM based voltage measurement results with the first ICs set

First ICs set								
Power supply voltage (V)	Measured LPF2 voltage V_m (V)	Converted power supply voltage using LPF method (V)	Voltage error in LPF method (mV)	Voltage error percentage in LPF method (%)	Measured duty cycle (%)	Converted power supply voltage using duty cycle (V)	Voltage error in duty cycle method (mV)	Voltage error percentage in duty cycle method (%)
16	0.615	16.11	105.14	0.66	17.76	15.75	-254.71	1.59
16.8	0.668	16.89	91.69	0.55	19.37	16.53	-273.40	1.63
16.85	0.67	16.92	71.37	0.42	19.46	16.57	-279.73	1.66
16.9	0.674	16.98	80.74	0.48	19.57	16.62	-276.34	1.64
16.95	0.678	17.04	90.10	0.53	19.68	16.68	-272.96	1.61
17	0.681	17.08	84.62	0.50	19.78	16.73	-274.43	1.61
18	0.748	18.08	78.94	0.44	21.82	17.72	-284.45	1.58
19	0.815	19.07	73.26	0.39	23.92	18.73	-265.35	1.40
20	0.881	20.05	52.74	0.26	25.92	19.71	-294.77	1.47
21	0.946	21.02	17.37	0.08	28	20.71	-285.38	1.36
22	1.015	22.04	41.37	0.19	30	21.69	-314.80	1.43
23	1.082	23.04	35.69	0.16	32.05	22.68	-319.96	1.39
24	1.148	24.02	15.17	0.06	34.1	23.67	-325.12	1.35
24.8	1.203	24.83	31.40	0.13	35.78	24.49	-309.84	1.25
24.85	1.205	24.86	11.08	0.04	35.88	24.54	-311.31	1.25
24.9	1.209	24.92	20.44	0.08	35.98	24.59	-312.79	1.26
24.95	1.212	24.96	14.97	0.06	36.04	24.62	-333.67	1.34
25	1.216	25.02	24.33	0.10	36.2	24.69	-306.02	1.22
26	1.283	26.02	18.65	0.07	38.25	25.69	-311.18	1.20
27	1.35	27.01	12.97	0.05	40.25	26.66	-340.61	1.26
28	1.417	28.01	7.29	0.03	42.3	27.65	-345.77	1.23
29	1.486	29.03	31.29	0.11	44.3	28.62	-375.20	1.29
29.8	1.538	29.80	3.00	0.01	46	29.45	-350.21	1.18
29.85	1.542	29.86	12.36	0.04	46.1	29.50	-351.68	1.18
29.9	1.546	29.92	21.72	0.07	46.2	29.55	-353.15	1.18
29.95	1.55	29.98	31.08	0.10	46.3	29.60	-354.62	1.18
30	1.552	30.01	10.76	0.04	46.44	29.66	-336.68	1.12

The conversion shows a maximum 105.14mV higher voltage than the actual power supply voltage with LPF conversion method having maximum 0.66% error. On the other hand, the duty cycle conversion method results in a maximum of 375.2mV lower voltage than the actual power supply voltage, and the maximum error conversion is 1.66%. The measured value V_m increased 2mV–4mV and the duty cycle increased 0.03%–0.07% with 50mV increase in power supply voltage.

Then all ICs were changed with the same models except resistors and capacitors. The measurement results of the second ICs set are shown in table 6.

Table 6. PWM based voltage measurement results with the second ICs set

Second ICs set								
Power supply voltage (V)	Measured LPF2 voltage V_m (V)	Converted power supply voltage using LPF method (V)	Voltage error in LPF method (mV)	Voltage error percentage in LPF method (%)	Measured duty cycle (%)	Converted power supply voltage using duty cycle (V)	Voltage error in duty cycle method (mV)	Voltage error percentage in duty cycle method (%)
16	0.632	16.36	357.43	2.23	18.24	15.98	-21.78	0.14
16.8	0.685	17.14	343.98	2.05	19.9	16.78	-16.20	0.10
16.85	0.688	17.19	338.50	2.01	20	16.83	-17.67	0.10
16.9	0.693	17.26	362.71	2.15	20.1	16.88	-19.14	0.11
16.95	0.695	17.29	342.39	2.02	20.2	16.93	-20.61	0.12
17	0.699	17.35	351.75	2.07	20.3	16.98	-22.08	0.13
18	0.768	18.38	375.75	2.09	22.4	18.00	-2.98	0.02
19	0.833	19.34	340.39	1.79	24.42	18.98	-22.70	0.12
20	0.9	20.33	334.71	1.67	26.51	19.99	-8.45	0.04
21	0.968	21.34	343.87	1.64	28.56	20.99	-13.61	0.06
22	1.035	22.34	338.18	1.54	30.62	21.99	-13.92	0.06
23	1.102	23.33	332.50	1.45	32.7	23.00	-4.53	0.02
24	1.169	24.33	326.82	1.36	34.72	23.98	-24.25	0.10
24.8	1.224	25.14	343.05	1.38	36.37	24.78	-23.52	0.09
24.85	1.226	25.17	322.73	1.30	36.5	24.84	-10.44	0.04
24.9	1.231	25.25	346.94	1.39	36.6	24.89	-11.91	0.05
24.95	1.232	25.26	311.78	1.25	36.7	24.94	-13.38	0.05
25	1.235	25.31	306.30	1.23	36.8	24.99	-14.85	0.06
26	1.304	26.33	330.30	1.27	38.85	25.98	-20.01	0.08
27	1.371	27.32	324.62	1.20	40.9	26.97	-25.17	0.09
28	1.44	28.35	348.62	1.25	42.95	27.97	-30.34	0.11
29	1.506	29.33	328.10	1.13	44.96	28.95	-54.91	0.19
29.8	1.559	30.11	314.65	1.06	46.6	29.74	-59.04	0.20
29.85	1.564	30.19	338.85	1.14	46.7	29.79	-60.51	0.20
29.9	1.566	30.22	318.53	1.07	46.82	29.85	-52.28	0.17
29.95	1.57	30.28	327.89	1.09	46.95	29.91	-39.19	0.13
30	1.573	30.32	322.42	1.07	47.05	29.96	-40.66	0.14

In the second ICs set, the average difference between the converted power supply voltage and the actual voltage is 336mV, and the error ranged from 1.06% to 2.23% in the case of LPF method. However, the error decreases from the first ICs set if the duty cycle conversion method is used. The maximum error is 0.2% with the duty cycle method.

4.2 LED Circuits

A program for 3kHz PWM signals was not available at the time of the measurements. The Arduino was used to generate 732Hz PWM signals that had 2.85V high level voltages. It was not possible to achieve 100% PWM duty cycle with the program used in Arduino. The maximum duty cycle was 99.61% which is considered to indicate the full brightness at 21V in the calculation. The subcircuit was disconnected from the power, and the PWM pins of Arduino were connected to the corresponding pads on the subcircuit for the measurements.

The LED cards had 10mA emergency current with the original resistor values. The 3000K LED channel was measured by keeping the 5000K LED branches at 10mA emergency current because the measured values would also be close if the measurements were taken at 13mA emergency current.

4.2.1 3000K LED Channel

The LED branches' characteristics were first measured at 21V. Measurements were taken by keeping the emergency mode on for the 5000K LED channel. The voltage across the D1 diode was 0.93V. The maximum 65.96mA current was observed on the sixth branch, and the minimum current was measured to be 64.26mA on the second branch at 21V full brightness. This results in 2.58% difference between the minimum and maximum LED branch currents. The average LED voltage was 2.828V at 21V full brightness. Only measurement results of the fourth branch, which draws power approximately from the midsection of the VDS net on the PCB, are shown in table 7.

Table 7. LED branch currents at different brightness levels at 21V of the 3000K LED channel

Brightness level (%)	PWM duty cycle (%)	Resistor voltage (V)	Average LED current (mA)	Theoretical LED current (mA)
100	99.61	0.305	64.894	
70	69.53	0.214	45.532	45.121
50	49.6	0.152	32.340	32.187
30	29.7	0.091	19.362	19.273
10	9.77	0.0312	6.638	6.340
1	0.78	0.004	0.851	0.506

The LED branch current was measured by measuring the voltage across a 4.7Ω resistor. Theoretically, the LED current should be 66.73mA at 99.61% PWM duty cycle, according to the equation (11). The measured current was 64.894mA at 99.61% PWM duty cycle. The theoretical LED current values at different brightness levels are listed in the last column of table 7 by taking 64.894mA as the maximum current at 21V full brightness. The result shows that the average LED current and the PWM cycle have a good linear relationship.

Then the average LED voltages and D1 diode voltage drops at 99.61% PWM duty cycle were measured from 22V to 30V with 1V step leaving the 5000K LED channel on emergency mode. The results are shown in table 8.

Table 8. D1 diode and LED voltage drops from 22V to 30V

Power supply voltage (V)	D1 diode voltage drop (V)	Average LED voltage (V)
22	0.936	2.875
23	0.975	2.912
24	1.04	2.949
25	1.06	2.986
26	1.1	3.016
27	1.13	3.05
28	1.11	3.087
29	1.2	3.118
30	1.18	3.147

The voltages across the D1 diode and LED generally increased with higher power supply voltages. With D1 diode and LED voltage drop information from table 8, the required PWM duty cycles can be calculated for different brightness levels from 22V to 30V as per subsection 3.2.1. Theoretical PWM duty cycles and the measured PWM duty cycles for 24V and 30V are shown in table 9. The low PWM resolution of Arduino prevented the generation of exact duty cycles to achieve the theoretical current values; therefore, the measured PWM cycles refer to the approximate values that are required to achieve the theoretical currents.

Table 9. Theoretical and measured PWM duty cycles at different brightness levels at 24V and 30V of the 3000K LED channel

Brightness level (%)	Target LED current (mA)	24V		30V	
		Theoretical PWM duty cycles (%)	Measured PWM duty cycles (%)	Theoretical PWM duty cycles (%)	Measured PWM duty cycles (%)
100	65	57.138	58.6	30.3	31.64
70	45.5	39.997	40.62	21.194	21.88
50	32.5	28.569	29.3	15.138	15.62
30	19.5	17.141	17.19	9.083	9
10	6.5	5.714	5.08	3.028	2.35
5	3.25	2.857	2.34	1.514	1.17

The measurements show that the theoretical and measured PWM duty cycles to achieve the desired brightness levels are close. It is observed that lower PWM duty cycles than the theoretical ones were needed to achieve low brightness, such as 10% or lower brightness at both 24V and 30V power supply.

It was possible to control the 3000K LED channel using the full range of the PWM duty cycle because the gate voltages of the MOSFETs could exceed the MOSFETs' threshold voltages at very low PWM duty cycles. The optocoupler's emitter reached about 11V during PWM on time.

4.2.2 5000K LED Channel

The LED current and voltage drop characteristics of the 5000K LED branches were similar to the 3000K LED branches in switch mode. The emergency circuit required $R_{EN} = 18k\Omega$ and 150Ω , 1000Ω , 2200Ω resistors in parallel with the internal 95Ω emitter to ground resistor of the constant current IC to limit the current to 13mA in emergency mode. The emergency mode currents through each branch at 24V and 30V are shown in table 10.

Table 10. LED branch currents in emergency mode

Branch	24V	30V
	Current (mA)	Current (mA)
1	13.3	13
2	13.26	12.89
3	13.1	12.85
4	13.1	12.84
5	13.1	12.87
6	13.3	12.97

Measurement results show that the current remained almost equal throughout the voltage range and branches. Table 10 shows that the current decreased a little with the increase in the power supply voltage. The current starts to decrease after about 17.8V and maintains about 5.9mA at 16.8V.

The emergency mode turned on below 0.78% PWM duty cycle with $C_3 = 100$ nF and $R_3 = 1M\Omega$. The Optocoupler's emitter high level voltage was 4.71V, and capacitor C_3 voltage was 3.98V at 0.78% PWM duty cycle. These voltages reduce to 2.22V and 1.62V respectively at 0.39% PWM duty cycle which turn off LED branch MOSFETs and Q3 MOSFET, and the emergency mode is turned on.

The emitter voltages of the optocouplers from both LED channels had similar waveforms. The 3000K LED channel optocoupler's emitter had higher top voltage than the 5000K LED channel optocoupler's emitter at low duty cycles, such as less than 5%. Both optocouplers had similar characteristics at the

higher duty cycles. The top voltage of the 5000K LED channel optocoupler reached about 11V. The emitter voltage waveforms of the 5000K LED channel optocoupler at 49.61% and 0.78% are shown in figure 39 and 40 respectively. The yellow wave represents the PWM signal, and the green waveform represents the optocoupler's emitter voltage.



Figure 39. The emitter voltage waveform of the 5000K LED channel optocoupler at 49.61% PWM duty cycle



Figure 40. The emitter voltage waveform of the 5000K LED channel optocoupler at 0.78% PWM duty cycle

The optocoupler has difficulties lining up with the PWM signal at very low and high duty cycles. The waveform looks better at other duty cycles. The optocoupler stays on longer than the PWM signal at very low duty cycles and does not turn off fully at duty cycles approximately higher than 98.83%.

Branch 3 was connected to the midsection of the VDS net on the PCB. Measurement results are shown for this branch. Table 11 shows the measurement results at 21V. The 3000K LED channel was turned off during the measurements.

Table 11. LED currents at different brightness levels at 21V of the 5000K LED channel

Brightness level (%)	PWM duty cycle (%)	Resistor voltage (V)	Average LED current (mA)	Theoretical LED current (mA)
100	99.61	0.313	66.596	
69.53	69.53	0.219	46.596	46.304
49.6	49.6	0.156	33.191	33.031
29.7	29.7	0.094	20	19.779
9.77	9.77	0.0325	6.915	6.506
0.78	0.78	0.0037	0.787	0.519

Theoretical currents are calculated based on the 66.596mA maximum current. The measured current values are close to the theoretical ones. Table 12 shows the measurement results at 24V and 30V with 3000K LED channel in off condition. Theoretical values are calculated using the LED and D1 diode voltage drops found for the 3000K LED channel.

Table 12. Theoretical and measured PWM duty cycles at different brightness levels at 24V and 30V of the 5000K LED channel

Brightness level (%)	Target LED current (mA)	24V		30V	
		Theoretical PWM duty cycles (%)	Measured PWM duty cycles (%)	Theoretical PWM duty cycles (%)	Measured PWM duty cycles (%)
100	65	57.138	57	30.3	31.64
70	45.5	39.997	39.85	21.194	21.88
50	32.5	28.569	28.13	15.138	15.23
30	19.5	17.141	16.8	9.083	9
10	6.5	5.714	5.08	3.028	2.34
5	3.25	2.857	2.34	1.514	1.17

Table 12 shows that the measurement results are close to the 3000K LED channel results in table 9. However, both 3000K and 5000K LED branches deviate from the results shown in table 7 and 11 when both channels operate at the same brightness levels. The deviation is within 2mA current. The results are shown in table 13 at 21V. The currents through the branches reduced in this measurement. For example, it was 64.894mA at full brightness, but the new measurement shows the current is 62.979mA for the 3000K LED branch. Similarly, the 5000K LED branch current reduces to 64.468mA from 66.596mA at full brightness.

Table 13. 3000K and 5000K LED channel characteristics at 21V when both LED channels were operating

Brightness level (%)	PWM duty cycle (%)	3000K LED branch		5000K LED branch	
		Resistor voltage (V)	Average LED current (mA)	Resistor voltage (V)	Average LED current (mA)
100	99.61	0.296	62.979	0.303	64.468
69.53	69.53	0.208	44.255	0.212	45.106
49.6	49.6	0.148	31.489	0.151	32.128
29.7	29.7	0.088	18.723	0.091	19.362
9.77	9.77	0.0306	6.511	0.0315	6.702
0.78	0.78	0.004	0.851	0.0038	0.809

There is noticeable voltage change across the D1 diode when both channels operate at considerable brightness. This voltage change contributes to the

deviation. Another D1 diode voltage drop measurements were taken from 21V to 30V by keeping both LED channels turned on at 99.61% PWM duty cycles. The results are shown in table 14.

Table 14. D1 voltage drop from 21V to 30V with both channels on at 99.61% PWM duty cycles

Power supply voltage (V)	D1 diode voltage drop (V)
21	1.036
22	1.09
23	1.106
24	1.2
25	1.26
26	1.35
27	1.4
28	1.48
29	1.57
30	1.7

5 Discussion

The LED circuits mostly followed the theoretical calculations. There were some differences among the LED branch currents due to the components' tolerances and undesired voltage drops along the PCB traces. The measurements were taken with 732Hz PWM signals. It is expected to see more non-linearity between the PWM duty cycle and the brightness level when the LEDs are driven with 3kHz PWM signals because of the slow response of the standard optocoupler. This may be mitigated by using the high speed optocouplers.

Both 3000K and 5000K LED types have maximum continuous current rating of 180mA and 240mA pulsed current with duty cycle equal to or less than 10%, according to the datasheets. The maximum current through the fourth branch of the 3000K LED channel was measured to be 210mA at 30V supply voltage keeping the 5000K LED channel in emergency mode. This exceeds the maximum continuous LED current rating but is within the range of 240mA pulsed current. However, the duty cycle should not exceed 10% if the LEDs are driven with 240mA pulsed current. For a safer operation, each branch may

contain five LEDs. For example, the required resistor value for five LEDs per branch is $\frac{21V-5 \times 2.828V-0.93V}{65mA} = 91.23\Omega$ according to equation (12) with updated D1 diode and LED voltage drop at 21V. This makes the LED current approximately $\frac{30V-5 \times 3.147V-1.18V}{91.23\Omega} = 143.43mA$ at 30V supply voltage, which is lower than the maximum continuous LED current limit.

The emergency mode turned on below 0.78% PWM duty cycle. The CTR degradation of the optocoupler is expected to cause emitter voltage reduction which may turn on the emergency mode above 0.78% PWM duty cycle in the future. Retriggerable monostable multivibrator ICs like 74LS123 can be utilized to solve this issue. The EN pins of the constant current ICs can be connected to the output of the 74LS123. The 74LS123 can then be configured into the retriggering mode that checks if the PWM signal is available from the optocoupler. If the PWM signal is available, the output of 74LS123 is low, and the 5000K LED branches operate in switch mode. The 74LS123 outputs high when the PWM signal is missing and turns on the emergency mode.

The linear optocoupler based voltage measurement results show that the difference between input and output photodiode currents may seem small but it causes significant voltage measurement error, and IL300 IC to IC variation impacts the result heavily. This method does not fit with this thesis work application. A further measurement can be done with the HCNR201 linear optocoupler.

The maximum error voltage is 348.62mV, above 21V, which occurs at 28V in PWM based voltage measurement using the LPF method with the second ICs set. The actual LED current at 28V is $\frac{28V-6 \times 3.087V-1.11V}{46.3\Omega} = 180.73mA$, this would require $\frac{65mA \times 100}{180.73mA} = 35.96\%$ PWM duty cycle to achieve full brightness. This PWM based voltage measurement circuit would require erroneously $\frac{65mA \times 100}{1000} \div \frac{28.348V-6 \times 3.087V-1.11V}{46.3\Omega} = 34.53\%$ PWM duty cycle, which is 1.43% lower than the actual duty cycle. The same circuit with different batch ICs of the same models

can be measured to determine what offset voltage can be used in the equation to lower the measurement error. This circuit is the slowest among all the voltage measurement circuits discussed in this thesis. As described in subsection 3.1.4, the PWM would saturate when there is a significant sudden change in the power supply voltage. Therefore, the average of the samples is recommended when the voltage is measured using the duty cycle. LPF method alleviates this issue highly; however, it would take about two seconds to settle the measurement with 300k Ω resistors and 1 μ F capacitors for the low pass filters. It was tested that frequencies lower than 0.53Hz do not produce any noticeable measurement accuracy. If a large Rf value, such as more than 560k Ω , is used with the U1 error amplifier, a Cf capacitor value that forms a low pass filter around 60Hz is required to make U1 stable. This circuit can be built with modern op-amps and high speed optocouplers to see how much improvement they make. This PWM method is expected to produce more accurate measurements if the feedback can be taken out of the LPF2.

TL431 based voltage measurement circuit produces \pm difference with the actual voltage depending on the LED card. The error percentage is generally less than 2%. More CTR values on more LED cards can be measured which may reduce the error in all LED cards overall. The measurements were taken with only the emergency mode on. It will cause more inaccuracy when both LED channels operate because the voltage drop across the D1 diode will increase. One calculation for the LED current difference between LED card 1 and card 2 is provided. Assume only the 5000K LED channel is operated with full brightness at 24V, and the 3000K LED channel is off. According to table 3 and 4, LED card 1 measures 24V as 24.27V whereas LED card 2 measures 23.64V. Table 8 states that the D1 diode voltage drop is 1.04V, and the LED voltage drop is 2.949V. The LED card 1 microcontroller calculates the PWM duty cycle to be $\frac{65mA \times 100}{1000} \div \frac{24.27V - 6 \times 2.949V - 1.04V}{46.3\Omega} = 54.36\%$. Similarly, LED card 2 microcontroller calculates a 61.34% PWM duty cycle. These calculations make the actual LED current on the LED card 1 be $\frac{54.36 \times 1000}{100} \times \frac{24V - 6 \times 2.949V - 1.04V}{46.3\Omega} = 61.83mA$, and similarly, the actual current on LED card 2 is 69.77mA. There is a 7.94mA

current difference between these two LED cards at full brightness at 24V with only the 5000K LED channel on. If the microcontroller measures decimal voltage values, such as 25.3V, the calculations can be performed using the nearest data points from tables 8 and 14.

The isolation amplifier technique provided the best result among all techniques. The error is less than 0.61%. It provides the least measurement error in IC to IC variation. This method suits this thesis work application well if the cost is not an issue.

The use of the D1 diode as reverse voltage polarity protection does not fit well for the LED driving technique used in this thesis work. The high voltage drop across the D1 diode affects the current through the LED branches and the voltage measurement. If the D1 diode can be removed, then the LED branches and the voltage measurement circuit are not required to depend on the voltage drop. No separate diode voltage drop measurements would be required, as shown in tables 8 and 14. There should be other methods to protect the LED card against the reverse voltage polarity that does not cause a significant voltage drop. One method could utilize the MOSFETs as the protector [30]. For example, if MOSFET's $R_{DS(on)}$ is 20m Ω and the current is 2A, then the voltage drop is 40mV, which can be ignored in the LED and voltage measurement circuit equations.

The LED branch requires many resistors of small values if one single resistor does not meet the power dissipation rating. It requires significant space on the PCB. Further studies can be performed to see if this LED driving technique with all limitations benefits overall more than the other techniques for specific applications.

6 Conclusion

The purpose of this thesis work was to design an LED driving circuit with PWM signals through the isolation barrier. The circuits were built upon LED cards, which are the single units of the lighting system, provided by Teknoware company, in public transport. Two color temperature LEDs, 3000K and 5000K, were used in the LED cards. Each LED type consisted of 36 LEDs that were divided into six parallel branches where each branch contains six LEDs. There is a subcircuit that includes a microcontroller. The subcircuit is separated from the main circuit with isolation. The microcontroller controls the 3000K and 5000K LED channels separately by manipulating PWM signals. The power supply voltage varies from 16.8V to 30V. Both LED channels have nominally 65mA LED branch current at 21V. The microcontroller controls the brightness level by varying the PWM duty cycle. The brightness and the PWM duty cycle have a linear relationship. The LED branches were configured in switch mode through N-channel MOSFET switches. The microcontroller generated PWM signals drive the MOSFETs' gates. The higher power supply voltage than 21V requires the PWM duty cycle to be less than 100% to generate a 65mA average current through the LED branches. The information on the power supply voltage is vital because the required PWM duty cycle depends on the power supply voltage level. The microcontroller measures this power supply voltage and determines what PWM duty cycle is required to achieve a specific brightness level. The 5000K LED channel enters the emergency mode at 20% brightness level when the PWM signal is missing on the 5000K LED channel.

There are isolated voltage measurement circuits available based on linear optocouplers and isolation amplifiers, but they were costly for this thesis work application. The majority of this thesis work was devoted to developing an isolated DC voltage measurement technique using the standard optocoupler on a tight budget. It was necessary to design a circuit that does not depend on the standard optocoupler's CTR for improved measurement accuracy. A PWM based isolated voltage measurement circuit was developed that does not depend on the optocoupler's CTR. It was presumed by the company that the

PWM based voltage measurement method may interfere with other signals. The company decided to use the TL431 IC using the standard optocoupler for the voltage measurement. Linear optocoupler and isolation amplifier based circuits were also built on breadboards to check their performances.

The isolated voltage measurement circuits were tested twice. The ICs were changed with the same models to observe how IC to IC variation affects the voltage measurement accuracy. Linear optocoupler, isolation amplifier, and PWM based circuits were built on breadboards for the measurements. Only the linear optocoupler and the isolation amplifier ICs were changed during their second tests. All ICs except the resistors and capacitors were changed during the second test for the PWM based voltage measurement circuit. TL431 based circuit was measured on two different LED card PCBs. The measurements of the 3000K and 5000K LED channels were taken only on one LED card.

The voltage information under 21V is not vital as the maximum PWM duty cycle is 100% at voltages lower than 21V. The summary of the voltage measurement circuits is stated for 21V to 30V. The linear optocoupler had the worst measurement result in IC to IC variation. The maximum error voltage percentage increased from 4.87% to 10.99% on the second test. The error voltage continued increasing with the increase in the power supply voltage. The maximum voltage difference between the measured and actual voltage was 3V at 30V supply voltage.

TL431 based measurement circuit had a maximum 3.22% error at 21V. The results showed \pm error voltage depending on the LED card. For example, LED card 1 and card 2 measured 24.27V and 23.64V respectively at 24V supply voltage.

There are two ways to measure the voltage in the PWM based voltage measurement circuit: by measuring the duty cycle of the PWM signal or by measuring the analog voltage. The circuit produced a maximum 0.19% and 1.43% error at 22V on the first ICs set when the analog voltage and duty cycle

methods were used respectively. However, on the second ICs set, the analog voltage method increased the maximum error percentage to 1.64%, and the duty cycle method reduced the maximum error percentage to 0.2%. The measurement results suggest that the error shall be around 350mV in either method in IC to IC variation. More circuits with ICs of the same models need to be tested to acquire more complete characteristics. A further test can be performed to see if this method interferes with other signals.

The isolation amplifier produced the least error among all the isolated DC voltage measurement techniques. It had maximum 0.61% error within the full power supply voltage range. Most measured values were within 100mV of the power supply voltage.

The LED channels shall be driven by 3kHz PWM signals. However, the program for 3kHz PWM signals was not available during the measurements. An Arduino generated 732Hz PWM signals were used for the measurements. Both 3000K and 5000K LED channels had similar characteristics in switch mode. The measured PWM duty cycles were close to the theoretical values at different brightness levels. The 3000K LED channel was controllable by the full range PWM duty cycle, however, the 5000K LED channel entered the emergency mode below 0.78% PWM duty cycle.

The use of a diode as reverse polarity protection affects the accuracy of both the voltage measurement circuit and the LED current because the equations depend on the diode voltage drop. The measurement results presented for the TL431 based voltage measurement circuit are based on the emergency mode operating condition. The measurement accuracy will be affected when the LED cards are operated in other conditions. Therefore, it is necessary to employ other methods for reverse voltage protection where the voltage drop can be neglected.

This thesis work implemented a PWM based LED driving method as an alternative to voltage regulated LED driver ICs. Further work can be carried out

to see how this PWM driving method performs against the LED driver ICs in terms of efficiency, cost, and PCB space. The software department of the company shall develop the program for the microcontroller based on this thesis work findings to drive the LED cards. The company shall install the LED cards on a tram and observe if this PWM approach would be beneficial.

References

- 1 LED Drivers [Internet]. Diodes Incorporated. [cited 2023 Aug 7]. Available from: <https://www.diodes.com/products/power-management/led-drivers/>
- 2 Why Do I Need Signal Isolation? [Internet]. Acromag. 2021 [cited 2023 Aug 7]. Available from: <https://www.acromag.com/blog/why-do-i-need-electrical-isolation-an-acromag-whitepaper/>
- 3 General Description [Internet]. Vishay Semiconductors. [cited 2023 Aug 7] p. 1. Available from: <https://www.vishay.com/docs/80059/80059.pdf>
- 4 Appel M, Kruck A. Guidelines for Reading an Optocoupler Datasheet [Internet]. Vishay Semiconductors. [cited 2023 Aug 7] p. 2. Available from: <https://www.vishay.com/docs/84256/useoptocouplerdatasheet.pdf>
- 5 Martins D, Bayer L. How to Use Optocoupler Normalized Curves [Internet]. Vishay Semiconductors. [cited 2023 Aug 7]. Available from: <https://www.vishay.com/docs/83706/applicationnote45.pdf>
- 6 TCMT110. Series Optocoupler, Phototransistor Output, Single Channel, Half Pitch Mini-Flat Package [Internet]. Vishay Semiconductors. [cited 2023 Aug 7]. Available from: <https://www.vishay.com/docs/83510/tcmt11.pdf>
- 7 Calculate Reliable LED Lifetime Performance in Optocouplers [Internet]. Broadcom. 2022 [cited 2023 Aug 7]. Available from: <https://docs.broadcom.com/doc/AV02-3401EN>
- 8 Koeck D. Lifetime of Optocouplers [Internet]. Würth Elektronik. 2021 Feb [cited 2023 Aug 7] p. 3. Available from: <https://www.w-online.com/components/media/o303314v410%20ANO006a%20EN.pdf>
- 9 Smat R. Introduction to comparators, their parameters and basic applications [Internet]. STMicroelectronics. 2012 [cited 2023 Aug 8]. Available from: https://www.st.com/resource/en/application_note/an4071-introduction-to-comparators-their-parameters-and-basic-applications-stmicroelectronics.pdf
- 10 Kugelstadt T. Active Filter Design Techniques. In: Op Amps For Everyone [Internet]. 2002 [cited 2023 Aug 9]. p. 1–63. Available from: https://web.mit.edu/6.101/www/reference/op_amps_everyone.pdf
- 11 Alter D. Using PWM Output as a Digital-to-Analog Converter on a TMS320F280x Digital Signal Controller [Internet]. Texas Instruments. 2008 Sep [cited 2023 Aug 9]. Available from: <https://www.ti.com/lit/an/spraa88a/spraa88a.pdf>

- 12 Karki J. Active Low-Pass Filter Design [Internet]. Texas Instruments. 2023 Feb [cited 2023 Aug 10]. Available from: <https://www.ti.com/lit/an/sloa049d/sloa049d.pdf>
- 13 ANALOG FILTERS . In: BASIC LINEAR DESIGN [Internet]. Analog Devices; 2007 [cited 2023 Aug 10]. p. 1–144. Available from: <https://www.analog.com/media/en/training-seminars/design-handbooks/Basic-Linear-Design/Chapter8.pdf>
- 14 Karki J. Analysis of the Sallen-Key Architecture [Internet]. Texas Instruments; 2002 Sep [cited 2023 Aug 11]. Available from: <https://www.ti.com/lit/an/sloa024b/sloa024b.pdf>
- 15 Analog Filter Wizard [Internet]. Analog Devices. [cited 2023 Aug 11]. Available from: <https://tools.analog.com/en/filterwizard/>
- 16 Filter Design Tool [Internet]. Texas Instruments. [cited 2023 Aug 11]. Available from: <https://webench.ti.com/filter-design-tool/>
- 17 Sallen-Key Low-pass Filter Design Tool [Internet]. OKAWA Electric Design. [cited 2023 Aug 11]. Available from: <http://sim.okawadenshi.jp/en/OPseikiLowkeisan.htm>
- 18 Buffer (Follower) Circuit [Internet]. Texas Instruments. 2019 Jan [cited 2023 Aug 12]. Available from: <https://www.ti.com/lit/an/sboa269a/sboa269a.pdf>
- 19 AN-31 amplifier circuit collection [Internet]. Texas Instruments. 2020 Oct [cited 2023 Aug 12]. Available from: <https://www.ti.com/lit/an/snla140d/snla140d.pdf>
- 20 TL431, TL432 Precision Programmable Reference [Internet]. Texas Instruments. 2022 Jul [cited 2023 Aug 12]. Available from: <https://www.ti.com/lit/ds/symlink/tl431.pdf>
- 21 Sedra AS, Kenneth Carless Smith. Microelectronic circuits. 7th ed. Oxford Oxford University Press; 2014.
- 22 AN90026 LED drivers [Internet]. Nexperia. 2021 Feb [cited 2023 Aug 13] p. 2. Available from: <https://assets.nexperia.com/documents/application-note/AN90026.pdf>
- 23 LED Drive Methods and Circuit Design [Internet]. STANLEY ELECTRIC CO., LTD. 2008 May [cited 2023 Aug 13] p. 3. Available from: https://www.stanleyelec-stj-components.com/data/technical_note/TN003_e.pdf
- 24 LCW MVSG.EC [Internet]. ams-OSRAM. 2021 Dec [cited 2023 Aug 14] p. 14. Available from: https://dammedia.osram.info/media/resource/hires/osram-dam-5584202/LCW%20MVSG.EC_EN.pdf

- 25 Görk D, Kruck A. Designing Linear Amplifiers Using the IL300 Optocoupler [Internet]. Vishay Semiconductors. 2021 Oct [cited 2023 Aug 15]. Available from: <https://www.vishay.com/docs/83708/appnote50.pdf>
- 26 AMC1311x High-Impedance, 2-V Input, Reinforced Isolated Amplifiers [Internet]. Texas Instruments. 2022 Jun [cited 2023 Aug 16]. Available from: <https://www.ti.com/lit/ds/symlink/amc1311.pdf>
- 27 TL494 Pulse-Width-Modulation Control Circuits [Internet]. Texas Instruments. 2022 Jun [cited 2023 Aug 17]. Available from: <https://www.ti.com/lit/ds/symlink/tl494.pdf>
- 28 AVR135: Using Timer Capture to Measure PWM Duty Cycle [Internet]. Microchip Technology Inc. 2016 Apr [cited 2023 Aug 17] p. 6. Available from: https://ww1.microchip.com/downloads/en/Appnotes/Atmel-8014-Using-Timer-Capture-to-Measure-PWM-Duty-Cycle_ApplicationNote_AVR135.pdf
- 29 CNY17 Optocoupler, Phototransistor Output, with Base Connection [Internet]. Vishay Semiconductors. 2014 Jan [cited 2023 Aug 18]. Available from: <https://www.vishay.com/docs/83606/cny17.pdf>
- 30 Huang A, Roth E. 11 Ways to Protect Your Power Path [Internet]. Texas Instruments. 2019 Apr [cited 2023 Sep 5] p. 33. Available from: <https://www.tij.co.jp/lit/eb/slyy168/slyy168.pdf>

Additional PWM Based Voltage Measurement Results

The measurements were obtained without U4A buffer. Vx voltage from the voltage divider was connected to the non-inverting terminal pin 1 of U1 op-amp. Both low pass filters had the same component values with 300kΩ resistors and 4.7μF capacitors. Other variations of LM324 were used for the low pass filters. Table 15 shows the measurement results for the standard and high speed optocouplers at 1.27kHz frequency. All other components were the same for each test. The measurements were taken by the multimeter.

Table 15. Comparison between standard and high speed optocoupler result

Multimeter taken measurements				
Power supply voltage (V)	Standard optocoupler		High speed optocoupler	
	Converted power supply voltage (V)	Error voltage (mV)	Converted power supply voltage (V)	Error voltage (mV)
16	15.996	-4.36	15.966	-34.23
17	17.041	41.06	16.981	18.68
24	24.240	239.53	24.016	-15.51
25	25.270	270.02	25.031	-31.06
29	29.317	317.29	29.004	-3.66
30	30.333	332.84	30.004	-4.28

The voltage difference was between 4.36mV and 332.84mV with the standard optocoupler. The high speed optocoupler improves the result to less than 34.23mV difference with the power supply voltage.

Table 16 shows the result when the circuit was operated at 408Hz with the standard optocoupler. The measurements were taken with the multimeter.

Table 16. Measurement results of the standard optocoupler at 408 Hz

Multimeter taken measurements		
Power supply voltage (V)	Standard optocoupler	
	Converted power supply voltage (V)	Error voltage (mV)
16	15.861	-138.77
17	16.877	-123.22
24	23.927	-72.60
25	24.941	-58.54
29	28.959	-41.14
30	29.974	-25.59

The operation at 408Hz improves the result for the standard optocoupler. Now, the voltage difference is between 25.59mV and 138.77mV. However, the measured voltage is less than the actual power supply voltage as opposed to table 15.

Then the measurements were taken by the Arduino and for the second ICs set as well. Table 17 shows the measurement results at 408Hz.

Table 17. Comparative result for two ICs sets with the standard optocouplers at 408Hz

Measurements taken with multimeter				
Power supply voltage (V)	First ICs set		Second ICs set	
	Converted power supply voltage (V)	Error voltage (mV)	Converted power supply voltage (V)	Error voltage (mV)
16	15.801	-198.51	15.607	-392.66
17	16.787	-212.83	16.593	-406.98
24	23.762	-238.38	23.687	-313.05
25	24.807	-192.96	24.658	-342.30
29	28.839	-160.62	28.690	-309.96
30	29.885	-115.20	29.586	-413.89

The use of Arduino produces more voltage error than the multimeter. There is about 100mV more voltage than the measurements taken with the multimeter. However, the error voltage difference is about 200mV between the two sets of ICs unlike the result seen in tables 5 and 6 in the main report where it was about 300mV.